Implications for the Resilience of Modern Coastal Systems Derived from Mesoscale Barrier Dynamics at Fire Island, New York

Daniel J. Ciarletta[1], Jennifer L. Miselis[1], Julie C. Bernier[1], Arnell S. Forde[1]

[1]U.S. Geological Survey, St. Petersburg Coastal and Marine Science Center, 600 4th St. S, St. Petersburg, Florida 33701, USA

Correspondence to: Daniel J. Ciarletta (dciarletta@usgs.gov)

Abstract. Understanding coastal barrier response to future changes in rates of sea-level rise rate, sediment availability, and storm intensity/frequency is essential for coastal planning, including socioeconomic and ecological management. Identifying drivers of past changes in barrier morphology, as well as barrier sensitivity to these forces, is necessary to accomplish this. Using remote-sensing, field, and laboratory analyses, we reconstruct the mesoscale (decades-centuries) evolution of central Fire Island, a portion of a 50-kilometer barrier island fronting Long Island, New York, USA. We find that the configuration of the modern beach and foredune at Fire Island is radically different from the system's relict morphostratigraphy. Central Fire Island is comprised of at least three formerly inlet-divided rotational barriers with distinct subaerial beach and dune-ridge systems that were active prior to the mid-19th century. Varying morphologic states reflected in the relict barriers (e.g., progradational, transgressive) contrast with the modern barrier, which is dominated by a tall and nearly continuous foredune and is relatively static except for erosion and drowning of fringing marsh. We suggest this state shift indicates a transition from a regime dominated by inlet-mediated gradients in alongshore sediment availability to one where human impacts exerted greater influence on island evolution from the late 19th century onward. The retention of some 'geomorphic capital' in Fire Island's relict subaerial features combined with its static nature renders the barrier increasingly susceptible to narrowing and passive submergence. This may lead to an abrupt geomorphic state shift in the future, a veiled vulnerability that may also exist in other stabilized barriers.

1 Introduction

Barrier coasts, including barrier islands, spits, and strandplains, front portions of every continent on Earth. Among these landforms, sandy barrier islands are commonly located along the subtropical to subpolar coasts of passive continental margins (Davis, 1994; McBride et al., 2022), including the east coast of North America (Leatherman, 1979a). The eastern seaboard of Canada, the United States, and Mexico contains nearly 4,300 km of barrier islands (Stutz and Pilkey, 2001), and the almost continuous stretch of barriers within the United States is among the largest reaches of barrier islands in the world (Zhang and Leatherman, 2011). Despite their ubiquity, efforts to assess barrier morphologic resilience and future evolution in the face of rising seas and increasing storm frequency/intensity (Seneviratne et al., 2021) are complicated by (1) their diverse present-day

geomorphology, and (2) a lack of insight regarding the relative importance of the various mesoscale (decades to centuries) drivers of morphologic state change shifts under different environmental conditions (Cooper et al., 2020; Vousdoukas et al., 2020). Here, we describe morphologic resilience as the capacity of the coastal landscape to maintain the distribution and character of its subaerial ecomorphological features through time (Masselink and Lazarus, 2019), with state shifts comprising

35   threshold changes in system morphology that cannot be easily recovered to a previous configuration (Kombiadou et al., 2019).

Field and modeling studies have demonstrated that mesoscale barrier dynamics, defined here as barrier-lagoon behavior at decadal/centennial timescales and meter to kilometer spatial scales (Cooper et al., 2018; Sherman, 1995), are significantly primarily controlled by sediment accommodation and availability (Brenner et al., 2015; Ciarletta et al., 2021; Cooper et al., 2018; Psuty, 2008; Raff et al., 2018; Shawler et al., 2021a). These drivers are in turn a function of antecedent

40   topography (e.g., pre-transgressive surface morphology; Shawler et al., 2021a), inlet dynamics (Nienhuis and Lorenzo-Trueba, 2019), climate and vegetation (Jackson et al., 2019; Mendes and Giannini, 2015), and inherited relict or "inherited" morphology (relict barrier morphological features; Timmons et al., 2010). The latter overlaps with the concept of geomorphic capital, which is defined as sediment reserves that must be exhausted before frontal erosion of a barrier transitions to wholesale migration (Mariotti and Hein, 2022). Mesoscale barrier dynamics also include human interventions, which have impacted

45   coastal barriers directly and indirectly for decades to hundreds of years through manipulation of sediment input and partitioning across the entire shoreface-barrier-marsh-lagoon system (Abam, 1999; Elko et al., 2021; Hein et al., 2019; Rogers et al., 2015; Tenebruso et al., 2022; Williams et al., 2013), as well as through stabilization and destruction of barrier geomorphic boundaries, such as the backbarrier-marsh interface (Stutz and Pilkey, 2005; Tenebruso et al., 2022).

The net morphological effects of mesoscale barrier dynamics are manifested through several key barrier behaviors.

50   We define these behaviors according to Robbins et al. (2022), including concepts such as seaward/alongshore growth (progradation/elongation), cross-shore/alongshore erosion (narrowing/shortening), as well as differential erosion and progradation (barrier rotation). Modeling allows for the investigation of future morphologic states stemming from these behaviorsbased on the interaction of natural and human drivers, though such efforts are usually limited due to a lack of historical data to constrain input parameters. Particularly for semi-natural and developed barriers, this means that information

55   concerning the natural balance of forces affecting system morphology must be gleaned from the geomorphic record. One approach is to decode the record of barrier state change from relict subaerial morphology (Ciarletta et al., 2019c, 2021), a process which is more regularly applied in strandplain systems (Bristow and Pucillo, 2006; Nooren et al., 2017; Oliver et al., 2019). Barrier islands can also retain an abundance of relict features, and recent attention has been placed on their importance in illuminatingwhich have been used to illuminate past evolution and drivers of morphologic change (Billy et al., 2013, 2014;

60   Raff et al., 2018; Shawler et al., 2019, Shawler et al., 2021b). Such efforts typically include conventional morphostratigraphic investigations in the form of core analyses and ground-penetrating radar scans, which can provide additional sedimentological and structural information to help reconstruct past barrier environments.

Here, we use geomorphic mapping of active and remnant dune features at Fire Island, a semi-natural barrier island in New York, USA, to gain insight into both natural and anthropogenic drivers of barrier landscape change. Although Fire Island

65 has been the subject of numerous field investigations and modeling studies (Leatherman, 1985; Lentz and Hapke, 2011; Locker et al., 2017; Schmelz and Psuty, 2022; Schwab et al., 2000; Schwab et al., 2014; ~~Ziegler~~Zeigler et al., 2022), little is known about the island's internal structure or the timing of its development, especially in its central ~24 km. This presents a variety of issues for forward modeling and management practices. Without a baseline of past morphologic variability, it is not clear what the natural character and distribution of ecologies in the Fire Island system were prior to significant human interference

70 in the landscape, or what the most important drivers were in shaping the barrier. Subsequently, it is not known how resilient the system was in the past, and whether the current system reflects a significant morphologic state shift from a previous configuration or is currently in transition to a new state. To fill the knowledge gap, we ~~New~~synthesize existing studies with ~~geomorphic mapping and~~ historical documentation of the island's landscape and new geomorphic mapping ~~identifies~~ to reveal locations where significant records of morphologic change are preserved. Ground-penetrating radar investigations coupled

75 with coring and radiocarbon dating then provide chronological control and paleoenvironmental information. ~~In total,~~Finally, combining this information, we reconstruct the evolution of central Fire Island to understand differences between present and past morphologic states, including how such differences could affect the system's future resilience and the implications for mesoscale behavior of barrier systems globally.

2 Background

80 **2.1 Study Setting**

Fire Island is a west/southwest-oriented, 50-km long barrier island located on the south coast of Long Island, New York, USA (Figure 1). It is bound to the west by Fire Island Inlet and to the east by Moriches Inlet. Fire Island was an unbroken barrier for 74 years (Leatherman and Allen, 1985), until Hurricane Sandy breached it in 2012 and created Wilderness Inlet 13 km west of Moriches Inlet. West of Wilderness Inlet, Fire Island is separated from Long Island by the kilometers-wide Great South

85 Bay, which is predominantly an open water lagoon with limited fringing marsh, especially along the barrier margin. To the east of Wilderness Inlet, approximately 7 km of the island fronts the mainland Mastic Peninsula and is backed by the constricted lagoon of Narrow Bay. Further east, the backbarrier lagoon widens again, and the island fronts about 4 km of Moriches Bay, divided from the updrift Westhampton barrier by Moriches Inlet.

Fire Island is part of a regional system of occasionally mainland-attached barriers referred to as the South Shore

90 Beaches or Great South Beach (hist.) that extends westward from glacial outwash headlands along the southeast coast of Long Island (Leatherman, 1985; McCormick et al., 1984). The direction of elongation along the South Shore Beaches reflects an east to west net littoral transport direction, which is primarily driven by cyclonic storms tracking northeasterly through and offshore of the Mid-Atlantic Bight (Hapke et al., 2010; Leatherman, 1985; van Ormondt et al., 2020). The area is microtidal, with a range of about 1.3 m (Leatherman, 1985).

95 Study area framework geology reflects Long Island's glacial origins. Nearly all Long Island surficial geology is composed of Laurentide Ice Sheet (LIS) sediments deposited during the Wisconsin glaciation (Fuller, 1914). Deposits in the

study area exist within a broad glacial outwash plain that extends southward from a succession of roughly east-west oriented moraines that define the central and northern portions of Long Island. Most notable are the Ronkonkoma and Harbor Hill moraines (Fuller, 1914), the former being active approximately 24 kya as the LIS reached its maximum extent (Figure 1; Balco and Schaefer, 2006). Digital elevation models depict two broad glacial outwash channels that descend from the Ronkonkoma moraine towards the coast in the vicinity of Fire Island (Figure 1), also identified by Fuller (1914). A channel underlying the Connetquot River appears to extend beneath the westernmost portion of the island, whereas another channel underlies the Carmans River and aligns with Wilderness Inlet (Figure 1) and was detected beneath the barrier shoreface there (Locker et al., 2017). Portions of Fire Island that do not overlie the glacial channels are thought to rest on antecedent topographic highs which could have acted as pinning points during late Holocene transgression (Locker et al., 2003; Shawler et al., 2021a). This is supported by well logs that identified glaciofluvial sediments within just a few meters of the surface of eastern Fire Island (Schubert, 2010) and by seismic studies in the central part of the island that identified a probable submerged topographic high—here referred to as the Central Submerged Headland (Figure 1)—potentially partly outcropping in the shoreface (Schwab et al., 2014). The latter may act as a source of sediment to adjacent shoreface-attached ridges (Figure 1) and ultimately the subaerial barrier (Schwab et al. 2014).

Although Schwab et al. (2014) identified a potential local source of sediment to Fire Island, it is thought that most of the sand moving through the modern barrier system comes from ~~the~~ littoral sediment supply (Kana, 1995; Leatherman and Allen, 1985). From Montauk to Shinnecock, the southeasterly section of the Ronkonkoma moraine is exposed to coastal bluff erosion where it actively sources sediment to the South Shore Beaches (Leatherman and Allen, 1985). Earlier in the Holocene, it is thought that ancestral barriers were further offshore, and ~~it is thought that~~ they derived sediment from deposits in now-submerged portions of the glacial outwash plain. The remnants of these ancient barriers are found 8 km offshore of modern Fire Island in the form of meters-thick sandy deposits arranged parallel to the coast (Sanders and Kumar, 1975). These deposits are composed of presumed lower shoreface sand that was left stranded on the continental shelf as sea level increased rapidly (Sanders and Kumar, 1975; Rampino and Sanders, 1980), possibly in association with a glacial meltwater pulse immediately preceding the 8.2-kyr global cooling event (Hijma and Cohen, 2010). Whether this ancient system survived drowning ~~and transgressed to the position of the modern barrier~~and maintained a portion of sediments derived from offshore deposits while undergoing transgression remains unknown (Rampino and Sanders, 1981, 1982, 1983). ~~Sediment cover overlying the transgressive unconformity between the modern and ancient system is thin, except for the succession of km-scale shoreface-attached ridges along the western end~~ of Fire Island ~~(Schwab et al., 2013, 2014).~~

2.2 Recent Geomorphic Change at Fire Island

Fire Island's surface geomorphology is strongly influenced by the local alongshore transport gradient (Figure 2) and was previously divided into four distinct zones based on surface geomorphic features (Ciarletta et al., 2021). Here, we supplement previous geomorphic feature interpretations with additional insights regarding barrier behavior over the last ~200 years ~~(Leatherman and Allen, 1985)~~. On the updrift (eastern) end of the island, the morphology is low-relief and transgressive

130 (Leatherman and Allen, 1985), featuring a single overwashed dune line (Figure 2a; Zone I). Conversely, the downdrift (western) end is historically elongational and contains the remnants of numerous poorly developed beach-ridge and recurved foredune ridge~~are~~s (Figure 2e; Zone IV) that formed in succession with a westerly-migrating spit end (Leatherman and Allen, 1985). In the central region of the island (Figure 2c/d: Zones II and III), as many as 1 to 4 shore-sub/parallel relict foredune ridges are seen in combination with the active foredune (Lentz and Hapke, 2011). The relict dunes are generally around 2-5

135 meters in elevation (NAVD88), potentially indicative of an environment that was formerly subject to combinations of spatially variable progradation and amalgamation. Conversely, the modern foredune system comprises a mostly continuous ridge up to 8 m in elevation that appears to be either largely stable or aggradational, especially when considering ~~the primarily~~ stable to slightly progradational decadal shoreline change trends observed in the latter part of the 20th century (Allen et al., 2002).

We interpret modern foredune morphology and elevation as indicative of a relatively immobile barrier island, which

140 is supported by the lack of inlet breaches in the central part of Fire Island since the early 1800s (Leatherman and Allen, 1985). Historically, the central region has been overwash-limited, subjecting the backbarrier to bayside shoreline erosion at a rate of 0.3 to 1.0 m/yr and resulting in island narrowing (Leatherman and Allen, 1985; Nordstrom and Jackson, 2005). Radiocarbon dating from an interdune bog a few kilometers east of Point O' Woods demonstrates that the west-central portion of the barrier has been relatively stable for as long as 400 years (Sirkin, 1972), and additional radiocarbon dates from relict flood

145 shoals/washover deposits beneath the central part of the barrier show that this section may have been near its modern position as early as 1100 years ago (Leatherman, 1985). Moreover, Clark (1986) suggests that Fire Island as a whole may have been relatively stable prior to the 18th century. Using age-controlled pollen data from cores taken from east of Watch Hill to Shinnecock Inlet, Clark (1986) demonstrates the presence of mature maritime forests on Fire Island and the updrift Westhampton barrier prior to this time, which is equated with a lack of inlet disturbance. However, the lack of geologic

150 investigations west of Watch Hill presents a critical knowledge gap in this interpretation.

~~Conversely, historical records s~~Since the 18th century, historical records show the updrift end of the island fronting the Mastic Peninsula has been overwashed and breached in numerous locations, and the most downdrift 8 km of Fire Island has elongated westward since at least 1825, with spit-end shoreline~~s is~~ well documented in nautical charts, land surveys, and other historical accounts (Leatherman and Allen, 1985; Ruhfel, 1971; Taney, 1961). Low relief and poorly developed recurved

155 dunes were noted to exist 8 km updrift of the 1825 spit-end shoreline (Leatherman and Allen, 1985; McCormick, 1984), suggesting westward elongation of the island likely occurred prior to the 19th century. This 16-km section of elongation is believed to have originated from the area of Point O' Woods, where the morphology transitions to a shore-subparallel succession of relict dune ridges interspersed with mature maritime forest—the latter being indicative of a long period of relatively stable conditions (Leatherman and Allen 1985; Ruhfel, 1971; Sirkin, 1972,). This interpretation is consistent with

160 the evolution of Fire Island Inlet, which is thought to have migrated westward from the vicinity of Point O' Woods around the 1680s (Ruhfel, 1971; Suydam, 1942), although no scientific investigations have previously been undertaken to validate this.

Although reliable records~~evidence~~ indicate~~s~~ long-term barrier stability in central Fire Island, particularly in Zone III, other authors suspected this section of the barrier was much more dynamic ~~than observed historically~~prior to extant historical

observations (Leatherman and Allen, 1985; McCormick et al., 1984). Regardless of the exact nature and temporal framework of its stability, the relative longevity of this section of the barrier (Figure 2c/d; Zones II and III) suggests it contains a long-term, prehistoric geomorphological record of past changes in sediment fluxes and environmental forcing that could be used to develop a baseline of Fire Island's natural morphologic variability and resilience. In this study, weBased on this assessment, we leveraged this stability and collected comprehensive geologic data from Zzones II and III. Along with similar data from adjacent areas of Zones I and IV, and combining our new data with past studies and historical observations, we (1) determine the timing of relict ridge and beach formation in Zones II and III, (2) identify the drivers of changes in sediment availability that influenced island evolution, and (3) infer possible evolutionary pathways for Fire Island and other barriers in the future. On the last point, the presence of relict ridge successions in central Fire Island also compels us to consider the impacts that geomorphic capital might have in the future, especially since this is an emerging area of concern that has been poorly described and quantified until recently (Hein and Mariotti, 2022).

3 Observations and Methods

3.1 Geomorphic Interpretation

We first assessed central Fire Island's geomorphology using lidar digital elevation models (DEMs) from 2020 (U.S. Army Corps, 2021) and 2014 (Brenner et al., 2016), with additional information about long-term geomorphic change derived from historical shorelines (see Allen et al., 2002;, Himmelstoss et al., 2010;, and Terrano et al., 2020) and other observational/mapping records (McCormick et al., 1984; Strong, 2018). This work guided subsequent field investigations and age control analyses and provided detailed geomorphic context for previous observations. Both lidar datasets have a horizontal grid resolution of 1 m and centimeter-scale vertical accuracy (Brenner et al., 2016; U.S. Army Corps, 2021).

DEMs spanning the study area were mosaicked in ArcGIS and shaded from 0 to 4 m elevation (NAVD88) to highlight the structure of relict dune ridge features, which are generally lower than the modern foredune system (see Figures 2 and 3). Trends of relict and active dune ridges in central Fire Island were hand-digitized as line segments, highlighting the presence of former inlets as well as the general structure of relict island platforms and modern accretional environments. In combination with ground-penetrating radar (GPR) data (see next subsection), the extent of relict island platforms, former inlet fills, and the modern foredune-beach system were also hand-digitized. These features were combined with geochronological data from radiocarbon analyses and historical observations to produce a morphochronological map of central Fire Island (Figure 4).

3.2 Morphostratigraphic Investigations

GPR data from 2021 (Forde et al., 2023) and 2016 (Forde et al., 2018a/b) were used to characterize the morphostratigraphy of specific sites. Subsurface profiles were acquired using a GSSI SIR-3000 GPR system with a 200 MHz antenna and differential GPS position control. Radar wave velocity corrections were applied to profiles based on hyperbola analyses to determine dielectric constants, rendering depth-adjusted profiles for subsequent elevation correction and interpretation. Where position

195 fixes were absent, elevation corrections were applied to depth-adjusted profiles by using topography from 1-m lidar DEM grids (see Brenner et al., 2016; U.S. Army Corps, 2021). For raw/processed data and detailed methods for 2016 profiles see Forde et al. (2018a/b); for the 2021 profiles see Forde et al. (2023).

To verify stratigraphy, characterize the subsurface depositional environments, and acquire dateable material, two sediment coring techniques were employed. Cores C1 to C4 (Figure 3b/d) were obtained using a vibracore system consisting
200 of a Dreyer 2-1/8" vibrator head powered by an 8-horsepower motor. Core tubes used by this system consisted of 3" diameter aluminum irrigation pipe. Cores C5 to C9 (Figure 3a/c) were obtained with an AMS 1-1/4" x 36" stainless steel sand probe, or "sand auger," which uses 1" diameter clear plastic core tubes for sediment recovery. Position control was accomplished using a differential GPS receiver. All cores were split, sampled, and described in the Sediment Core Laboratory at the U.S. Geological Survey, St. Petersburg Coastal Marine and Science Center, Florida. Core descriptions utilized Munsell soil charts
205 to characterize color and were photographed using a Nikon D80 digital single-lens reflex camera.

Core sections were sampled for grain-size analysis and age control based on core descriptions and comparison with GPR transects. For grain size, sediment samples were run through both a mechanical sediment sieve and a laser particle sizer, producing parallel analyses. For the sieve analysis, samples were sorted from clay to coarse sand, with no further sieving above 2 mm diameter. For the laser particle sizer, the fraction of sediment with sub 1 mm diameter was analyzed. Data shown in this
210 study depict the sub 1 mm grain size distributions from the laser particle sizer normalized to the total mass of each sediment sample. Raw and processed grain-size data, as well as core descriptions, images, and technical methods are available in Bernier et al. (2023).

.

3.3 Age Control

215 Age control was obtained for selected organic-rich sediment samples by accelerated mass spectrometry (AMS) radiocarbon dating—a full list of samples and calibrated ages can be found in Section 4.3. Radiocarbon samples were processed using both the organic sediment fraction and plant remains, with analyses performed by Beta Analytic, Inc., in Miami, Florida. For each sample, we report not only the conventional ^{14}C radiocarbon age, but also the isotope ratio mass spectrometer (IRMS) $\delta^{13}C$ with respect to VPDB (Vienna Pee Dee Belemnite), as well as and calibrated age ranges. Calibrated ages are based on terrestrial
220 calibration curves from INTCAL20 (Reimer et al., 2020) using the High Probability Density (HPD) Range Method (Ramsey, 2009).

For plant remains and organic sediment fraction, we perform an environmental interpretation based on the observed/modeled relationship between $\delta^{13}C$ and salinity in marsh sediments. In estuarine systems along the northeast coast of North America, decreasing salinity generally results in a progressive increase in $\delta^{13}C$ depletion (Chmura and Aharon, 1995).
225 This occurs due to the increasing presence of plants utilizing C-3 photosynthesis rather than C-4 photosynthesis in upland environments. C-3 plants generally have $\delta^{13}C$ in the range of -23 to -34 ‰, while C-4 plants range from -9 to -17 ‰ (Chmura and Aharon, 1995 c.f. Smith and Epstein, 1971). For organic sediments, this interpretation relies on the assumption of minimal

contribution from algae, which display a wider range of $\delta^{13}C$ values than plants across all salinity levels (Malamud-Roam and Ingram, 2001; Tanner et al., 2007). However, since we report $\delta^{13}C$ for both the organic sediment fraction and plant remains, this allows for a more robust interpretation than would be possible with organic sediment alone.

4 Results and Interpretation

4.1 Morphochronological Mapping

Relict dune ridge structure in central Fire Island reveals an updrift-downdrift morphologic dichotomy (see Figure 4 morphochronological mapFigure 4; compare b with c/d). From the Wilderness Inlet to Davis Park (Zone II; Figure 4b), the major barrier morphology consists mostly of two large (5-8 m elevation) shore-parallel dune ridges that gradually amalgamate westward into a single dune ridge. At the western end of Zone II, around Watch Hill, there are several prominent recurved ridges preserved in the barrier interior, with evidence of seaward truncation. These recurves abruptly end at a km-wide low point in island topography partly backed by a discontinuous ridgeline (Figure 4c). Downdrift of this low point, moderate-elevation relict dune ridge successions dominate the barrier platform within Zone III.

Focusing onWithin Zone II, historical shorelines show that the bifurcation of the foredune ridge in the updrift direction is related to inlet processes, with the eastern end of the Zone II barrier rotating seaward ('rotational barrier'—see Leatherman et al., 1982; McBride et al., 1995) after a previous iteration of the Wilderness Inlet known as Old Inlet closed in 1825, along with the closure of an immediately adjacent updrift inlet channel known as Smith Inlet in 1834 (Leatherman and Allen, 1985; McCormick et al., 1984; Figures 4b and 5). Shoreline surveys (Himelstoss et al., 2010) and historical change analyses (Allen et al., 2002) confirm seaward progradation and amalgamation in Zone II persisted until about the 1930s, with subsequent gradual retreat and relative stability consistent with local aggradation (Allen et al., 2002; McCormick et al., 1984). This aggradational phase was interrupted by the (re)opening of Wilderness Inlet in 2012, which created a downdrift erosion shadow that has so far resulted in the destruction of the most seaward foredune ridge for about 2.5-km in the alongshore (Figure 5).

On the western end of Zone II, past inlet activity has been documented in the region surrounding Watch Hill. McCormick et al. (1984) identified a former inlet on the updrift side of Watch Hill, herein referred to as "Long Cove Inlet" (Figure 4), which was open between 1770 and 1827 (McCormick et al., 1984), overlapping in time with Old Inlet. This created an island between the two inlets for more than half a century, which we refer to as the "Wilderness Barrier" (Figures 4b and 15). McCormick et al. (1984) also identifies another inlet on the downdrift side of Watch Hill, corresponding with a low spot west of the recurved ridges, but they could not identify any historical sources to confirm when this inlet was active. More recently, a map from 1670 was identified as depicting an inlet at this location, adjacent to what was formerly a whaling station (Strong, 2018), and so we refer to this inlet as "Whalers Inlet" (Figure 4). Based on lidar DEMs, aerial images, and ground observations, we interpret that the Watch Hill Bbarrier originated as a recurved spit complex that elongated from the vicinity of Long Cove and migrated downdrift in association with Whalers Inlet (Figure 6). On the Immediately updrift side ofof what was likely the final position of Whalers Inlet, we also identify an arcuate succession of sub-meter elevation swash ridges is

260 ~~present~~surrounding a central high point, consistent with a relict washaround near the tip of the spit (Figure 6d). ~~These are distinct from larger 2-5 m elevation recurved dune ridges, and they ring a central high point, consistent with a washaround origin.~~

The inlet and spit complex at Watch Hill ~~would have been~~whereas likely part of an older iteration of the Wilderness Barrier pre-Long Cove Inlet. Its existence created a downdrift erosion shadow coincident with what we identify as an

265 overwash-impacted transgressive dune backing most of Davis Park (Figure 6b). This reworked and discontinuous dune line is equivalent to the heavily overwashed, low-relief ridge that presently exists on the downdrift side of modern Wilderness Inlet. ~~We note that the former~~The former transgressive dune at Davis Park also abuts a succession of relict foredune ridges to the west (Figure 6b), ~~with~~and this transition ~~defining~~defines the boundary between Zones II and III.

The updrift ~~In~~portion of Zone III (Figure 4c)~~, the island downdrift of the Whalers Inlet erosion shadow~~ features a

270 succession of at least two shore-parallel relict foredune ridges fronted by ~~the~~a modern foredune, which is amalgamated in some places with the ~~first of the~~ relict ridgelines (see section 4.2 for subsurface interpretation). Overlap of the modern foredune with the relict ridge field and overall barrier narrowing increases in the downdrift direction, until relict ridges almost entirely disappear about 3 km downdrift of Whalers Inlet. Beyond this point, the barrier widens slightly downdrift, and the modern foredune is backed by relict ridges, which gently recurve to the northwest for about 1.5 km before terminating at another low

275 spot near Fire Island Pines. We interpret this downdrift section of recurved ridges as the location of prehistoric island elongation associated with the migration of an inlet ~~which~~that we call "Pines Inlet." As with Whalers Inlet, the final location of Pines Inlet is preserved well in the modern morphology of the barrier, with a landward-offset ridge complex downdrift of the inferred inlet throat (compare Figure 4c/d with Figure 2d). We refer to the section of island bound by Pines Inlet and Whalers Inlet as the "Barrett Beach Barrier," named after the portion of National Park Service land near its midpoint (Figure

280 4c). Age control is lacking for Pines Inlet, so it is not clear if the Barrett Beach Barrier existed as a fully independent island west of Watch Hill, although ~~the layout of~~ its relict ridge system is distinct with respect to adjacent barriers.~~from both the extant Watch Hill and Wilderness barriers~~ We infer that ~~T~~the Barrett Beach Barrier is probably much older than either of the updrift barriers, as the modern lagoon shoreline is eroding into the base of the rearmost relict ridges. This process ~~has yet to become~~is not yet obvious in the Wilderness Barrier despite it being relatively impervious to overwash~~,~~ since it began rotating

285 seaward two centuries ago.

West of Pines Inlet, the barrier narrows to a point about 3 km downdrift at Sailors Haven (Figure 4d). Here, the modern barrier is backed by a single, discontinuous relict dune ridge, and the modern foredune is cut by a prominent washover channel. Island width increases downdrift of Sailors Haven, and the modern foredune is backed by an increasing number of relict dune ridges that recurve and splay gently towards the northwest and become truncated by the lagoon shoreline. The relict

290 ridges abruptly terminate at Point O' Woods, beyond which the barrier topography into Zone IV is dominated by a single foredune ridge backed by the remnants of low-relief recurved ridges associated with spit-building as Fire Island Inlet migrated westward. We refer to the section of island between Pines Inlet and the possible origin point of Fire Island Inlet as the "Sailors Haven Barrier." As with the Barrett Beach Barrier, ~~there is very little fringing marsh behind the Sailors Haven Barrier, and~~ the

lagoon shoreline is in many places cutting directly into the base of relict ridges, indicating this section of island has likely existed in its present location for centuries.

4.2 Subsurface Stratigraphy

Ground-penetrating radar scans within Zones II and III, specifically in the Wilderness, Watch Hill, and Sailors Haven barriers (see Figure 3 for layout), ~~confirm~~ support surface geomorphological interpretations and provide additional details on the cross- and along-shore structure of the island. Figure 7 shows the cross-shore structure of the Wilderness Barrier from the lagoon edge to the upper beach in Zone II at Ho-Hum Beach. Core C4, indicated in yellow, was acquired from the rear dune ridge, which was likely the primary foredune when Old/Smith Inlet closed in 1834 (see Allen et al., 2002). The relatively steep ~~ocean~~seaward-dipping reflections ~~seaward~~ shoreward of C4 confirm that progradation took place from this point to the shoreline's maximum seaward position in 1933 (Figure 5). Additionally, gently dipping reflections landward of C4 are consistent with washover deposition and ~~.~~ imply that the updrift portion of the Wilderness Barrier was transgressive prior to the episode of progradation inferred between 1834 and 1933.~~These observations imply that the updrift portion of the Wilderness Barrier was formerly transgressive and reached its most landward position in the early 19th century.~~

Figure 8 shows the alongshore subsurface structure ~~downdrift of Ho-Hum,~~ of the Watch Hill Barrier ~~Beach section of Zone II~~. In the updrift portion of this transect, reflections dip updrift, consistent with shore-subparallel erosion propagating from Long Cove Inlet (Figure 8, 700+ m). Further west, reflections become horizontal before reversing direction and dipping downdrift (Figure 8, 300 to 500 m). We associate this convex structure with a recurved barrier platform~~,~~ and demonstrate ~~we later confirm~~ that this platform is truncated in the cross-shore direction via core analysis (see Section 4.3). Another set of convex reflections partly onlap the tapering end of this "truncated beach" platform (Figure 8, 200 to 400 m), and we interpret these as comprising a discrete and bulbous recurved barrier platform, which we refer to as the "The Lobe." The horizontal extent of this feature is discernable in Figure 6. The ~~upper~~ surface of the lobe is dominated by swash-aligned washaround ridges (see Price, 1958) encircling a central high point about 200 m landward of the alongshore transect. Near the middle of the lobe, a borehole (S125990) from a previous study (Schubert, 2010) indicated the presence of the underlying transgressive surface at -5 m elevation. Reflections dipping downdrift from the truncated beach and partly underlying the lobe become horizontal at this elevation, corroborating Schubert's interpretation ~~and indicate the lobe is directly overlying the transgressive surface~~. Downdrift of the lobe, sharply concave reflections penetrate to an elevation of -6 to -7 m, consistent with a former inlet throat that scoured deep enough to excavate antecedent topography (Figure 8, 100 to 200 m). This feature likely marks the final position of Whalers Inlet before closure. Corresponding surface morphology depicts a remnant inlet slough abutting ~~a downdrift~~the transgressive ridgeline ~~consistent with an erosion shadow~~backing Davis Park (Figure 6b).

The transition from Zone II to III is marked by the appearance of surface successions of multiple relict sub/parallel dune lines beginning just west of Davis Park in the Barrett Beach Barrier (Figure 4c). Figure 9 depicts a cross-shore profile through this ridge field, revealing ~~an underlying~~a barrier platform characterized by seaward-dipping progradational reflections ~~signifying past beach progradation~~. Above these progradational beach/shoreface packages, discrete relict dune ridges are

evident. The modern foredune is ~~shown to be partly~~ amalgamated against the most seaward relict ridge and partly amalgamated with the second line of relict dunes through blowover deposition. ~~and~~It is also double the height of older dunes, which could be indicative of relatively prolonged barrier/beach stability or enhanced subaerial sediment availability.

330   Similar subsurface morphology is observed in the Sailors Haven Barrier in both the central (Figure 10) and downdrift (Figure 11) parts of the platform. The central area (Figure 10) reveals ~~is comprised of~~ tightly packed seaward-dipping reflections overlain by ~~a~~ an undulating surface that we interpret to represent a succession of short, partly buried dunes and/or berms. These short dunes are dwarfed by the modern amalgamated foredune, which rises to a heigh of 4 m over the otherwise relatively flat barrier surface. At the downdrift end of the platform (Point O' Woods), the subsurface structure is similarly

335 dominated by seaward-dipping reflections. We ~~, and in spots is overlain by~~infer that the base of relict dunes seen in subaerial morphology at Point O' Woods ~~that~~ are buried up to 2 m below the modern barrier surface (Figure 11). Approximately 75-100 m landward of the modern foredune, reflections also depict a shallow swale approximately 100 m in width, which is filled by washover sediments (see lithology results; section 4.3). Along the seaward margin of the swale, a 50 m-wide and 1.5-2 m thick interval of convex reflections ~~is consistent with~~ suggests the presence of a buried, overwash-impacted dune. A succession of

340 progradational packages that underlie the modern foredune offlap from this feature, which suggest that. ~~In total, that~~ these ~~results suggest that~~ Point O' Woods demonstrates at least two ~~sustained older and younger~~ episodes of progradation, possibly separated by an episode of ~~beach transgression~~ erosion that, at one point, ~~eroded the barrier to a position~~relocated the shoreline ~75 m landward of the modern foredune.

    Alongshore GPR transects at Point O' Woods depict only gently downdrift-dipping reflections consistent with the recurvature of surface dune ridge traces (Figure 4d). ~~Just downdrift in~~In Zone IV, ~~and beyond the mapped limit~~downdrift of

345 the Sailors Haven Barrier, alongshore reflections dip relatively steeply in both the seaward and downdrift directions, consistent with past spit growth (Figure 12). This supports historical accounts and morphological impressions ~~which indicate~~indicating that the 16 km of Fire Island within Zone IV comprise a spit that has grown westward from the vicinity of Point O' Woods.

4.3 Lithology and Environmental Interpretation

350 The lithology of Zone I ~~can be~~is characterized by ~~C~~core C5, recovered 2.5 km east of Wilderness Inlet at Smith Point (Figure 13; see Figure 3a for core location). Collected at the backbarrier-marsh interface, the bulk lithology of the core is consistent with a succession of washover deposits and primarily. ~~It primarily features~~consists of interbedded coarse to medium sand~~, but also at least one distinct unit displaying normal bedding (fining upward from coarse to medium sand)~~. Despite the core being just a few meters seaward of the marsh fringe ~~and penetrating more than a meter below the land surface~~, no marsh units were

355 recovered. ~~Since m~~Multiple marsh intervals ~~were~~ identified in cores from adjacent barriers ~~and~~ are believed to coincide with quiescent periods between extreme storms (Bennington and Farmer, 2015), and their absence in our core likely indicates more frequent washover consistent with the transgressive morphology of Zone I.

    In Zone II, the lithology from ~~C~~core C4 ~~confirms~~ supports our morphostratigraphic interpretation that the former foredune of the Wilderness Barrier was ~~in this location in the~~present at this location by the early ~~the~~ 19th century (Figure 13).

360 The upper 158 cm of the core is characterized by laminated fine-medium aeolian sand—finer than recovered in any other core. ~~Recovered~~ This dune sand overlies a 12-cm interval of medium-coarse sand and occasional shell fragments interpreted to be former beach/backshore. ~~L~~The l~~This l~~ithology correlates directly with the adjacent cross-shore GPR profile seen in Figure 7, which shows sub-horizontal reflections consistent with aeolian deposition overlying seaward-dipping reflections diagnostic of a former beach.

365 The lithology from ~~C~~Core C9, recovered from the throat of Long Cove Inlet, is consistent with inlet closure, and ~~dating confirms sediments overlap in time with when Love Cove Inlet is believed to have filled in, ultimately reconnecting the Wilderness and Watch Hill barriers~~is supported by age control (Figure 13). Specifically, the bottom 4 cm of the core consists of organic-rich sand, which is overlain by a deposit of interlaminated coarse and medium sands and a veneer of loose, medium sand with organic-rich horizons. Accounting for surrounding surface morphology (Figure 6), we interpret this sequence as a 370 vegetated inlet slough infilled by washover, the surface of which was subjected to aeolian reworking. Radiocarbon dating of the sediment component of the organic sand unit returned an age of 90 ± 30 yrs BP (c. 1860 CE), whereas plant remains within this unit returned 120 ± 30 yrs BP (c. 1830 CE). Including calibrated age ranges (Table 1), this overlaps with the historically documented timeframe for Long Cove Inlet's closure in 1827 CE (McCormick et al., 1984). Additionally, plant δ^{13}C was measured at -16.1‰, which in the U.S. northeast is consistent with a low marsh environment (Chmura and Aharon, 1995) and 375 suggests sediment at the bottom of the core was ~~at least briefly~~ under the influence of the Great South Bay before burial by washover.

The elongational spit complex of the Watch Hill Barrier was sampled by ~~Cores~~ cores C8, C7, and C6 (Figure 6). C8 targeted the seaward margin of the relict foredune on the "truncated beach" platform (Figure 8), while C7 and C6 targeted landward and seaward areas on "The Lobe" immediately downdrift. ~~C~~In general, ~~c~~ore lithologies and age control support the 380 interpretation that both platforms experienced seaward truncation coincident ~~in association~~ with the erosion shadow of Long Cove Inlet. Relict beach lithology is found in the upper part of ~~C~~Core C8~~.~~, including ~~Sediments between 23 and 43 cm consist of~~ alternating bands of dark reddish brown heavy-mineral sand and clean grayish sand, ~~with thinner alternating bands observed around 60 cm~~which we associate with post-storm beach rebuilding. This interpretation is partly informed by ~~Since~~ a similar sequence ~~was found~~observed on the modern beach after a late-season nor'easter impacted Fire Island on April 18 and 19, 2022~~, 385 just two days before C8 was acquired~~ (Figure 14)~~, these sediments likely represent post-storm beach rebuilding~~. Deeper lithological units within C8 demonstrate th~~at~~e~~at the~~ overlying s~~e~~ beach sediments ~~also~~ reflect shoreline transgression on the "truncated beach" platform. ~~Below the beach beds is~~These strata consist of a half-meter thick sequence of medium to coarse sand overlying two distinct layers of hemic peat separated by a thin sand bed. From the bottom up, this lithology is interpreted to record an episode of prolonged quiescence in a protected backbarrier environment—probably a drowned interdune and/or 390 inter-spit swale—which was interrupted by relatively rapid emplacement of washover due to shoreline retreat. Radiocarbon dating of organic sediments in the upper and lower peat layers return ages of 280 ± 30 and 260 ± 30 yrs BP (c. 1670 and 1690 CE), respectively, while plant material produces ages of 130 ± 30 and 180 ± 30 yrs BP (c. 1820 and 1770 CE). As with Core C9, plant δ^{13}C (Table 1) is consistent with a low marsh setting, while organic sediment δ^{13}C is ~~more~~ consistent with a high

marsh setting. ~~In both the plant and organic sediment fractions,~~ δ^{13}C becomes less depleted in the up-core direction~~,~~ for the plant and organic sediment fractions, ~~which suggests~~suggesting increasing salinity prior to washover emplacement. Subsequently, we posit that the youngest plant remains could represent the timeframe just prior to burial by washover. This assumption combined with an age comparison of plant remains for C8 and C9 (Table 1), suggest that the relict beach sediments in C8 reflect shoreward truncation of the Watch Hill Barrier resulting from the erosion shadow of Long Cove Inlet. This is further supported by a Coast and Geodetic Survey chart that shows a remnant indentation of the shoreline downdrift of the former Long Cove Inlet in 1835 (Leatherman, 1989).

Cores C6 and C7 (Figure 13) were used to explore the nature of "The Lobe" (Figure 6) discussed in previous sections. C6 penetrated the lobe at a more seaward position relative to C7, with its lithology comprising a thin veneer of likely wind-reworked sediment overlying a thick sequence of massive to faintly bedded medium to coarse sand interpreted as washover. This is consistent with alongshore GPR data (Figure 8) which indicate the relict lobe surface near C6 is mantled by ~2 m of transgressive sediment packages. With ~~Core c~~Core C7, we sought to recover sediment from the crest of a washaround ridge identified in aerial imagery on the lobe (Figure 6b/d). The top 23 cm of recovered section reveals a sequence of faintly laminated medium to coarse sand, which we equate with the ridge structure. Directly below this interval is a 24-cm thick unit of coarse sand, with mm- to cm-scale mud balls ~~(see Mukhopadhyay et al., 2022)~~ immediately below the upper contact (see Mukhopadhyay et al., 2022). We interpret this unit as reworked washover and marsh sediments flanking the subaerially exposed portion of the lobe. Finally, beneath the coarse sand interval is a sequence of centimeter-thick beds consisting of, from top to bottom, hemic peat, a thin bed of fine to medium sand, hemic peat, and more fine to medium sand, which we interpret as backbarrier marsh that was episodically buried by washover (Figure 13). Radiocarbon dating of organic sediments in the upper and lower peat layers return ages of 140 ± 30 and 270 ± 30 yrs BP (c. 1810 and 1680 CE), respectively, while plant material produces ages of 30 ± 30 and 180 ± 30 yrs BP (c. 1920 and 1820 CE). Ages for the lower peat layer in C7 are comparable to the upper peat layer of C8, and they are also at the same elevation. Intriguingly, while plant-derived δ^{13}C in the upper peat layer of C8 is indicative of a low marsh environment, C7's lower peat layer is relatively δ^{13}C depleted and consistent with a brackish fringe setting (Table 1). Taken together, this could reflect initial narrowing of the updrift portion of the Watch Hill ~~b~~Barrier ~~in the updrift direction as a~~in response to the opening of the Long Cove Inlet.

In Zone III, cores C1, C2, and C3 paralleled GPR line 18 (Figure 11). Core C1 penetrated the barrier's lagoon beach, C2 penetrated the interior relict dune system, and C3 targeted the area of the buried swale (Figure 13). The lithology and age of these cores illuminate a complex and relatively long sequence of morphologic change. For example, C1 records an entire cycle of barrier emplacement and drowning. Starting at the bottom, the core features an interval of medium to coarse sand that matches with seaward dipping reflections recorded in GPR data (Figure 11), suggesting a beach origin. Above ~~the inferred~~this ~~beach sand~~ lies a unit of deformed medium to coarse sand that we equate with the base of a relict dune, or maybe a deposit akin to a beach ridge as opposed to a true aeolian dune. The 39 cm of medium sand overlying this unit contains occasional root fragments and is likely the preserved surface of the rear dune flank. This is corroborated by a landward-dipping reflection seen in the GPR data (Figure 11).

Overlying the preserved dune surface at C1 is a 31-cm thick peat interval, which is overlain by a 34-cm thick washover deposit. Radiocarbon dating of the base of the peat returns an organic sediment age of 330 ± 30 yrs BP (c. 1620 CE), while dating of plant remains returns an age of 140 ± 30 yrs BP (c. 1810 CE). We assume the large discrepancy in age to represent contamination of older sediments with younger plant remains, but the difference is useful for inferring the longevity of the environment that produced the peat. Both the organic sediment and plant remains demonstrate δ^{13}C values below -28 ‰, consistent with a freshwater terrestrial origin in an upland bog and implying this environment persisted for multiple centuries. We note that this timeframe also matches the reported age of bog sediments analyzed by Sirkin (1972) in the nearby Sunken Forest, which yielded a date of 250 ± 80 yrs BP (c. 1700 CE). It is unclear precisely when the overlying washover sediments werewas deposited, but soil horizons in the top 14 cm of the washover showunit -indicate that a terrestrial environment may have been present for some time after bog burial. Above the washover unit is a medium sand interval with a distinct dark brown color and organic laminae which represents the modern lagoon beach as it actively truncates former back-barrier deposits.

Similar to C1, Ceore C2 reached the underlying surface of inferred beach/backshore sediments at an elevation of -1.5 m NAVD88. Fine to medium sand overlying these sediments are inferred to have a dune origin. Core C3 failed to penetrate as deep as C1 or C2, it but it did penetrate the washover deposit seen in our GPR data (Figure 11). The deposit was found to beis ~1.5 m thick and overlying overlies 18 cm of peat lying atop a unit of medium sand. This washover may be partly sourced from the remnants of a low, transgressive dune identified in the subsurface (Figure 11). Though C2 lacked age control, a radiocarbon sample taken from the peat unit in C3 produced the oldest ages reported in this study, with organic sediment dated to 690 ± 30 yrs BP (c. 1260 CE) and plant remains dated to 460 ± 30 yrs BP (c. 1490 CE). As with the radiocarbon sample from C1, comparatively young plants are presumably rooted in older organic sediments. Both the organic sediment and plant remains also demonstrate δ^{13}C values below -25 ‰, again consistent with a long-lived upland bog; in this case, occupying a large interdune swale. The age of 690 yrs BP at C3 implies that relict beaches and ridges landward of this location (e.g., at C1 and C2) are even older. This interpretation is supported further by the elevation of the C1/C2 beach-dune interface near -1.5 m, which demonstrates that aeolian deposition occurred at a time when sea level was lower than at present. Additionally, Aassuming the date of 460 ± 30 yrs BP is representative of plants that grew closer to the end of the peat's deposition, this sets a maximum age on the overlying washover unit and subsequent transgressive episode recorded in subsurface morphology.

5 Discussion

5.1 Timeline of Barrier Change at Fire Island

Our results demonstrate that the pre-20th century landscape of Fire Island featured successions of moderate-elevation progradational foredunes and low-elevation overwashed dunes distributed through time across a series of inlet-separated rotational and elongational barriers through time (Figure 15). Our investigation confirms some existing hypotheses about how the island evolved over the last six centuries. GPR and age-control data around Point O' Woods suggests the western spit of

460   Fire Island (Zone IV) began elongating from that location sometime after the late 16th century, which corresponds with the ~~historical timeline~~timeline proposed by historians (Ruhfel, 1971; Suydam, 1942; Figure 15c/d). Our GPR also confirms the presence of an inlet at Davis Park, which was inferred by McCormick (1984) and more recently documented from a historical map (Strong, 2018; Figure 15d/e).

Our data also reveal new information. Clark (1986) suggested Fire Island was generally a ~~more~~ relatively stable, inlet-
465   free barrier before the 18th century based on the inferred presence of mature maritime forest communities along the eastern half of the island prior to this time. However, our analysis suggests inlet activity was instead focused on the western side of the island between Watch Hill and Point O' Woods (Figure 15d/e), coinciding with a spatial data gap (Clark, 1986). We demonstrate not only the presence of the alongshore-migratory Whalers Inlet around Watch Hill, but also the presence of another inlet near Fire Island Pines. The impact of the latter on island morphology may be recorded at Point O' Woods, where
470   GPR profiles and radiocarbon dating suggests seaward truncation of the barrier occurred around or just after 1500 CE (Figure 15e).

This synthesis of present and past analyses shows that central Fire Island was subjected to spatially variable and sustained inlet activity between the 16th and early 19th century that drove alongshore ecogeomorphic heterogeneity. This contrasts with contemporary central Fire Island, which is dominated by a relatively static and continuous high-foredune system.
475   The change in barrier morphologic state from a diverse and dynamic landscape to a relatively stationary setting was suspected by earlier researchers (Leatherman, 1989; McCormick, 1984), but age control and morphostratigraphic relations among the various landscape components of the barrier were not understood well enough to conceptually describe the island's evolution. By seeking to confirm~~ing~~ impressions ~~of and providing chronological control for~~of past barrier behavior, we can move beyond local characterization and explore how inherited and modern morphology ~~and the geometry of the barrier's modern beach and~~
480   ~~foredune~~ might impact the resilience and evolution of the island in the future. Additionally, we can explore the implications of these findings for other barriers, as well as what ~~part~~ role human interventions play in ~~the fate of these systems based on~~ ~~past behavior~~modifying these systems. However, we first discuss the past drivers of sediment availability ~~in the~~at ~~past~~ Fire Island ~~system~~ to understand why the modern system appears as it does.

5.2 Inlets as Drivers of Barrier Morphologic Change: Then and Now

485   Changes in sediment availability are a primary driver of barrier behavior and geomorphic complexity ~~in barrier systems~~ (Brenner et al., 2015; Cooper et al., 2018; Psuty, 2008), and this work shows there were significant spatiotemporal variations in the sediment budget of Fire Island over the last 700+ years. All the relict barriers identified in this study—Wilderness, Watch Hill, Barrett Beach, and Sailors Haven—show evidence of differential progradation and transgression, as well as elongation and shortening. Most importantly, we demonstrate that these changes are related to the opening and closing of
490   inlets. This result is consistent with observations of modern barriers, which show that inlets can act as the primary driver of decadal-scale sediment redistribution ~~, as observed in the Malpeque barriers of eastern Canada~~ (Armon and McCann, 1979). Over longer timescales, even where overwash and other sediment transport mechanisms are active, sediment moved by inlets

can add up to most of the sand volume contained within individual barriers over the course of hundreds to thousands of years (Bartberger, 1976; Leatherman, 1989 c.f. Leatherman, 1987 and 1979b).

495   Our investigation shows inlet-mediated changes in the distribution of barrier sediments and destruction/creation of geomorphic capital (see Mariotti and Hein, 2022) were occurring at decadal to sub-centennial timescales and over kilometer-scale reaches. For example, radiocarbon dating of peat layers buried by washover deposits in the Watch Hill B̶b̶arrier confirms that the entire beach face of this former spit complex underwent significant t̶r̶a̶n̶s̶g̶r̶e̶s̶s̶i̶o̶n̶ erosion due to the opening of Long Cove Inlet in the early 19th century. Our geomorphic and lithostratigraphic analyses, combined with historical shoreline change

500   analyses from Allen et al. (2002), also confirm the closure of Old and Smith Inlets resulted in the seaward rotation of the entire 8-km shoreline of the Wilderness Barrier from the 1830s to the 1930s, creating the bifurcated dune system observed today.

        At Point O' Woods, our results show inlet-mediated changes in barrier morphology have occurred at the island-scale for hundreds of years. The formerly progradational landscape at Point O' Woods, likely reflecting past seaward rotation predating 690 yrs BP (c. 1260 CE), was disrupted by shoreline t̶r̶a̶n̶s̶g̶r̶e̶s̶s̶i̶o̶n̶ erosion probably resulting from updrift inlet

505   activity between 460 and 140 yrs BP (c. 1490 to 1810 CE). This may correspond with trends in the plan-view geometry of relict ridges that suggest there was an inlet at Fire Island Pines, midway between Davis Park and Point O' Woods (Figure 4c/d). Additionally, Fire Island's kilometer-scale elongation in Zone IV is believed to have begun around the 1680s (Ruhfel, 1971; Suydam, 1942). Since this is within the 460 to 140 yrs BP (c. 1490 to 1810 CE) window, it implies there could be a relationship between the erosion at Point O' Woods and the initiation of downdrift spit growth. We note that inlets can also

510   drive the liberation of sediments from antecedent topography (Shawler et al., 2019, 2021a), especially where this topography is relatively close to the surface. The spatial coincidence of previous inlets—e.g., Whalers Inlet (Figure 8)—and the Central Submerged Headland identified by Schwab et al. (2014) suggests that inlets excavated sediment that could have contributed to kilometer-scale island elongation in Zone IV.

        Given that Fire Island was once extensively modified by inlets, the question is: why not today? The lack of inlet

515   processes on modern Fire Island may relate to human development. Starting in the late 19th century, as interest in the island grew to include the establishment of communities and parks, it became progressively subject to coastal engineering. With the exceptions of Wilderness Inlet and Moriches Inlet,̶ ̶w̶h̶i̶c̶h̶ ̶w̶a̶s̶ ̶n̶a̶t̶u̶r̶a̶l̶l̶y̶ ̶f̶o̶r̶m̶e̶d̶ ̶i̶n̶ ̶1̶9̶3̶1̶ every breach that has developed in Fire Island since the 19th century has been mechanically closed. These include a recent breach through the barrier at Smith County Park (Zone I) after Hurricane Sandy (Bilecki, 2020), as well as multiple breaches in the eastern end of Fire Island

520   caused by the 1938 Long Island Hurricane (Howard, 1939). The two inlets currently bracketing the island, Fire Island Inlet and Moriches Inlet, were stabilized in the early-mid 20th century to prevent migration and closure (Leatherman and Allen, 1985; Ruhfel, 1971). Large-scale dune nourishment projects have also been undertaken, including efforts by the Works Progress Administration (WPA) to reconstruct 68 miles of dunes along the Suffolk County portion of the South Shore of Long Island beaches in 1939 (Morang, 1999). Studies have shown that even moderately tall (3 m) constructed dunes limit natural

525   overwash processes (Schupp et al., 2013), thus limiting inlet activity that might occur in areas of low/overwashed dune

topography (McCormick et al., 1984). The net effect is that morphologic change affected by inlets, at least on the spatiotemporal scales that Fire Island once permitted, may no longer be possible.

5.3 Inferring Future Morphological Evolution: Knowns and Unknowns

The impacts of human interventions and climate change in coastal barrier systems are creating scenarios for which there may
530 be no historical analogs, either ecological (Williams and Jackson, 2007) or purely morphological (Ciarletta et al., 2019a/b; Magliocca et al., 2011; Rogers et al, 2015). The combined influence of geomorphic capital and human stabilization presents a new and unknown challenge for coastal management, particularly since the volume and distribution of subaerial and subaqueous sand reservoirs present in modern barrier systems is loosely quantified at best. There is also limited understanding about the natural rates of change that are possible in modern systems, mainly due to a lack of data about past barrier evolution
535 for specific systems over decadal to centennial timescales. Even where such detailed assessments exist, as ~~now~~ does now for Fire Island, future biogeomorphological resilience will depend on the interaction of modern and relict morphology, which is a dynamic that is not well understood. For example, future biogeomorphological changes modeled at Fire Island demonstrate considerable uncertainty because the modern beach and foredune reflects decades of shoreline stabilization efforts that are likely masking natural morphologic shifts (Rice, 2015; Zeigler et al. 2022, c.f. Armstrong and Lazarus 2019). This masking
540 effect is obvious in other barrier systems from dune scale to island scale. Beach and dune nourishment amount to artificially replenishing capital (Mariotti and Hein, 2022), and in some cases, this has resulted in narrow barriers resisting morphological state changes that wider barriers have succumbed to over just a few decades. As an example, Hog Island (Virginia, USA), a natural barrier island, was as much as 2 km wide, but temporarily reverted to a narrow, transgressive state over the course of 50 years (Robbins et al., 2022). Conversely, narrow stretches of the Bogue Banks (North Carolina, USA) that were naturally
545 evolving towards a transgressive state have resisted morphological state change for decades due to anthropogenic dune maintenance activities and mechanical closure of breaches (Timmons et al., 2010), which contributes to uncertainty in our ability to apply both conceptual and numerical models to predict future evolution.

In addition to interactions between geomorphic capital and human alterations, understanding of mesoscale coastal behavior is further complicated by other barrier landscape controls that may interact with inlet activity, including the degree
550 to which these processes may change the distribution and frequency of inlet formation and closure. In particular, spatiotemporal variations in the rates at which dunes accumulate sediment, as well as the maximum heights they achieve, could directly affect barrier vulnerability to breaching (McCormick et al., 1984). Such variations are themselves the result of complicated interactions among biophysical processes, and models indicate morphological bistability of either low or high dune states can sometimes occur among similar combinations of storm magnitude/frequency and vegetative forcing, and potentially within the
555 same barrier (Goldstein and Moore, 2016). Another factor influencing inlet activity is the distribution of sediment in the shoreface and inner continental shelf. Along Fire Island, there is an east-west dichotomy in the availability of inner shelf sediments ~~which~~that may have enhanced or even dominated the updrift-transgressive/downdrift-accretional trend in barrier

surface morphology over centennial and longer timescales (Schwab et al., 2013, 2014). Yet, it is unclear whether inner shelf sediment distribution set the conditions for where inlets formed or is itself reflective of past inlet activity.

560   Regardless of the processes interacting or competing with inlet activity, our results suggest that if Fire Island were capable of sustaining inlets at the decadal scale—as it once did—it would display greater alongshore variability in subaerial morphology, likely leading to more heterogeneous responses to storms and sea-level rise, as well as an increased diversity of habitats. Instead, as sea level increases, the modern island with its nearly continuous foredune system is likely to undergo a combination of gradual frontal erosion and passive drowning of the interior, with eventual transition towards a flatter and

565 narrower state (~~Ziegler~~Zeigler et al. 2022)—the starting phases of which are already evident (Nordstrom and Jackson, 2005). We hypothesize that Fire Island's resilience will continue to decline due to the relatively great height of the modern foredune, which studies have indicated could create a feedback loop of island narrowing and marsh destruction caused by a lack of washover deposition in the backbarrier (Dolan, 1972; Lorenzo-Trueba and Mariotti, 2017, Miselis and Lorenzo-Trueba, 2017; Magliocca et al., 2011; Rogers et al, 2015). Loss of morphological resilience is likely to be exacerbated by reserves of naturally

570 available sediment in reaches of relict progradational dunes, which could enhance Fire Island's short-term resistance (see Kombiadou et al. 2019) against landward migration but ultimately increase the island's long-term committed retreat (Mariotti and Hein, 2022) and persistence in an eventual low-elevation/transgressive state. This process is evident at Ho-Hum Beach, where downdrift erosion related to Wilderness Inlet has partly destroyed the modern foredune but not resulted in any changes to either the backbarrier shoreline or the relict dune line (Figure 7). We note that the effect of shallow antecedent topography

575 at Ho-Hum Beach (Figure 7) may also be a contributing factor in pinning the barrier's position at that location, which may induce further retreat hysteresis.

        In the most extreme scenario, the combination of a tall, anthropogenically influenced foredune, an abundance of geomorphic capital, and the presence of shallow antecedent topography could lead to island instability in the future, in some parts of Fire Island and possibly elsewhere where similar conditions exist. Modeling studies show that lags in barrier response

580 to sea-level rise tend to result in a rapid stepping back when overwash~~washover~~ begins to consistently reach the backbarrier (Ciarletta et al., 2019a; Shawler et al., 2021a). This can result in barrier drowning due to a combination of subaerial sediment loss to an over-deepened lagoon and partial abandonment of the lower shoreface (Ciarletta et al., 2019a; Lorenzo-Trueba and Ashton, 2014). Such a scenario does not account for~~also consider~~ the possibility of an increase in storminess in combination with an increase in rate of sea-level rise, which process-based modeling has demonstrated can result in very rapid (decadal-

585 scale) drowning of barriers due to a failure of post-storm sediment recovery to balance losses from subaerial sand reservoirs (Passeri et al., 2020). Even if this extreme scenario proves unrealistic for Fire Island, an outcome where the island simply maintains a thinner, alongshore-dominated geometry will be detrimental to mature ecological communities. This is already being realized in the island's maritime forests as they gradually drown and erode (Art, 1976; Sirkin, 1972).

        It is important to note that management is not the same everywhere at Fire Island. In designated wilderness areas,

590 such as that between Watch Hill and Smith Point, the island can breach and form inlets (e.g., Wilderness Inlet), and some return to inlet-mediated barrier rotation has been observed. However, it is unclear whether discrete areas lacking human

intervention are enough to substantially alter the island's evolutionary trajectory. As of early 2023, Wilderness Inlet appears to be closing after ~10 years, a relatively short lifespan when compared with Long Cove Inlet and Old Inlet, which persisted for 50+ years and altered the morphology of the island over much larger reaches. This shortened lifespan likely resulted from updrift nourishment activities, which can interrupt natural inlet evolution due to elevated updrift sand fluxes (e.g., Ludka et al., 2018). Though further research is needed, this behavior implies that variability in management and geomorphic capital increasingly become a secondary control on barrier geomorphic evolution as the overall ability to sustain inlets diminishes in tandem with increasingly large and overwash-resistant dunes.

Finally, the history of Fire Island's human development follows a pattern that is similar to other barriers in the region (Tenebruso et al., 2022) and beyond (Dolan, 1972; Seminack and McBride, 2015), and there is some evidence of such systems previously experiencing a greater distribution of inlet activity than at present (e.g., Assateague Island, Maryland—Seminack and McBride, 2015; Northern Outer Banks—Mallinson et al., 2010). Because modern coastal management practices often seek to stabilize existing inlets and prevent new inlet formation, one of the most significant drivers of decadal-centennial barrier geomorphic variability is limited during a time when changes to other drivers (e.g., sea-level rise and storm frequency/intensity) are more uncertain than ever. A dearth of inlet activity potentially promotes a decadal-scale loss of geomorphic resilience and may also alter the longer-term retreat behavior of barriers through the restriction of flood-tidal shoal deposition, which provides a platform for barrier migration and stabilization, as well as a source of sandy sediment during future transgression (Nienhuis and Lorenzo-Trueba, 2019). At a global scale, this may be promoting a scenario of future barrier destabilization and possible drowning that becomes increasingly challenging to avoid beyond centennial time horizons.

6 Conclusions

We found that the central region of modern Fire Island comprises a set of at least three formerly inlet-divided rotational barriers with distinct subaerial beach and dune-ridge systems that were formed by ~~differential~~alternating periods of progradation and transgression. In particular, the central-eastern portion of the barrier reflects the most recent episode of island-scale inlet-mediated coastal change, having been a rotational barrier as late as the early 19th century. Meanwhile, the central-western section of Fire Island preserves a long-term record of geomorphic change, revealing cycles of inlet-associated progradation and transgression stretching back 700+ years.

In contrast to its past evolution, Fire Island has seen a decrease in sustained inlet activity and is fronted by a largely stable and nearly continuous foredune. We interpret this shift in morphodynamic state as a response to human alterations and suggest that the barrier is approaching a geomorphic tipping point. Specifically, lack of landward sediment transfer and loss of ability to generate new geomorphic capital is amplifying bay erosion and encroachment of the barrier platform, which is gradually depleting relict sand reservoirs and priming the island for a rapid state shift to transgression and possible drowning in the future. We emphasize that this process may make variations in sediment management along the island ineffective in changing evolutionary trajectories, although additional research is needed to explore this here and in other barriers.

Comparison of our findings at Fire Island with other barriers ~~will also be~~are also needed to understand the range of
625 rates at which inlets naturally open and close, as well as the rates at which they alter sediment distribution across the combined shoreface-barrier-backbarrier continuum. This will help isolate the relative importance and timescales of inlet activity across a spectrum of barriers, allowing for a more robust quantification of barrier vulnerability in the context of human development and other anthropogenic impacts. Ultimately, such endeavors could help prioritize where management activities can be altered to promote future resilience.

630 **7 Data availability**

Lithological descriptions, grain size analyses, core photos, core X-rays, radiocarbon data, geospatial control, and acquisition/processing methods relating to sediment samples can be found in Bernier et al. (2023). See: https://doi.org/10.5066/P91P1T88.

635 Ground-penetrating radar reports, scans, navigation files, and acquisition/processing methods are available via Forde et al. (2018a/b) and Forde et al. (2023). See: https://doi.org/10.3133/ds1078, https://doi.org/10.5066/F7P84B1P, and https://doi.org/10.5066/P97YW2UL.

8 Author contributions

D.C. conceptualized the investigation with J.M., and executed the investigation with J.B. and J.M. Data analysis and curation
640 was undertaken by D.C., J.B., and A.F. The original draft of the manuscript was written by D.C. and J.M., with critical feedback and editing from J.B. and A.F. All authors agreed on the final draft.

9 Competing interests

The authors declare no competing interests. Any use of trade, firm, or product names is for descriptive purposes only and does not imply endorsement by the U.S. Government.

645 **10 Acknowledgements**

We would like to acknowledge the considerable planning and assistance received in making this work possible, particularly during a pandemic. For assistance rendered in data acquisition and survey planning, we want to thank the U.S. Geological Survey (USGS) New York Water Science Center, including Mike Noll, Bill Capurso, Tony Chu, Chris Schubert, and Ron Busciolano, among others, as well as the staff of the National Park Service at Fire Island National Seashore, including Jordan
650 Raphael, Kelsey Taylor, Jason Demers, and Mike Bilecki. For assistance rendered in the laboratory, we want to thank our

colleagues Nancy DeWitt (core sampling, equipment training/loading), Cheyenne Everhart (grain size analysis), Jessica Jacobs (core Xx-rays), and Noreen Buster (core sampling). We also want to acknowledge the Point O' Woods Association and the Village of Bellport Beach for providing access to field sites. This work was made possible through the USGS Mendenhall Research Fellowship program and the USGS Coastal and Marine Hazards and Resources Program.

655 **11 References**

Abam, T.K.S.: Impact of dams on the hydrology of the Niger Delta, Bulletin of Engineering Geology and the Environment, 57(3), 239-251, 1999.

Allen, J.R., LaBash, C. L., August, P.V., and Psuty, N.P.: Historical and recent shoreline changes, impacts of Moriches Inlet, and relevance to Island Breaching at Fire Island National Seashore, NY—Technical Report NPS/BSO-RNR/NRTR/2002-7
660 National Park Service, Boston, http://npshistory.com/publications/fiis/shoreline-changes-2002.pdf, 2002.

Armon, J.W. and McCann, S.B.: Morphology and landward sediment transfer in a transgressive barrier island system, southern Gulf of St. Lawrence, Canada, Marine Geology, 31(3-4), 333-344, 1979.

Armstrong, S.B. and Lazarus, E.D.: Masked shoreline erosion at large spatial scales as a collective effect of beach nourishment, Earth's Future, 7(2), 74-84, 2019.

665 Art, H.W.: Ecological studies of the Sunken Forest, Fire Island National Seashore, New York (NPS Scientific Monograph No. 7), U.S. Department of the Interior, National Park Service, https://www.nps.gov/parkhistory/online_books/science/7/index.htm, 1976.

Balco, G. and Schaefer, J.M.: Cosmogenic-nuclide and varve chronologies for the deglaciation of southern New England, Quaternary Geochronology, 1(1), 15-28, 2006.

670 Bartberger, C.E.: Sediment sources and sedimentation rates, Chincoteague Bay, Maryland and Virginia, Journal of Sedimentary Research, 46(2), 326-336, 1976.

Bennington, J.B. and Farmer, E.C.: Recognizing past storm events in sediment cores based on comparison to recent overwash sediments deposited by superstorm sandy, in: Learning from the Impacts of Superstorm Sandy, Academic Pres, 89-106, 2015.

675 Bernier, J.C., Miselis, J.L., and Plant, N.G.: Satellite-Derived Barrier Response and Recovery Following Natural and Anthropogenic Perturbations, Northern Chandeleur Islands, Louisiana, Remote Sensing, 13(18), 2021.

Bernier, J.C., Everhart, C.S., Ciarletta, D.C., Miselis, J.L., and DeWitt, N.T.: Sediment data from vibracores and sand augers collected in 2021 and 2022 from Fire Island, New York: U.S. Geological Survey data release, https://doi.org/10.5066/P91P1T88, 2023.

680 Bilecki, M.S.: Fire Island National Seashore: A breach in the barrier island at the Otis Pike Fire Island High Dune Wilderness, Parks Stewardship Forum 36(1), https://doi.org/10.5070/P536146375, 2020.

Billy, J., Robin, N., Certain, R., Hein, C. and Berné, S.: Barrier shoreline evolution constrained by shoreface sediment reservoir and substrate control: The Miquelon-Langlade Barrier, NW Atlantic, Journal of Coastal Research, 65 (sp2), 2089-2094, 2013.

685 Billy, J., Robin, N., Hein, C.J., Certain, R. and FitzGerald, D.M: Internal architecture of mixed sand-and-gravel beach ridges: Miquelon-Langlade Barrier, NW Atlantic, Marine Geology, 357, 53-71, 2014.

Brenner, O.T., Hapke, C.J., Lee, K.G., and Kimbrow, D.R.: Terrestrial-based lidar beach topography of Fire Island, New York, June 2014: U.S. Geological Survey Data Series 980, https://dx.doi.org/10.3133/ds980, 2016.

Brenner, O.T., Moore, L.J. and Murray, A.B.: The complex influences of back-barrier deposition, substrate slope and
690 underlying stratigraphy in barrier island response to sea-level rise: Insights from the Virginia Barrier Islands, Mid-Atlantic Bight, USA, Geomorphology, 246,334-350, 2015.

Bristow, C.S. and Pucillo, K.: Quantifying rates of coastal progradation from sediment volume using GPR and OSL: the Holocene fill of Guichen Bay, south-east South Australia, Sedimentology, 53(4), 769-788, 2006.

Chmura, G.L. and Aharon, P.: Stable carbon isotope signatures of sedimentary carbon in coastal wetlands as indicators of
695 salinity regime, Journal of Coastal Research, 124-135, 1995.

Ciarletta, D.J., Lorenzo-Trueba, J. and Ashton, A.D.: Mechanism for retreating barriers to autogenically form periodic deposits on continental shelves, Geology, 47(3), 239-242, 2019a.

Ciarletta, D.J., Lorenzo-Trueba, J. and Ashton, A.D.: Interaction of sea-level pulses with periodically retreating barrier islands, Frontiers in Earth Science, 7, 279, 2019b.

700 Ciarletta, D.J., Shawler, J.L., Tenebruso, C., Hein, C.J. and Lorenzo-Trueba, J.: Reconstructing coastal sediment budgets from beach-and foredune-ridge morphology: A coupled field and modeling approach. Journal of Geophysical Research: Earth Surface, 124(6), 1398-1416, 2019c.

Ciarletta, D.J., Miselis, J.L., Shawler, J.L. and Hein, C.J.: Quantifying thresholds of barrier geomorphic change in a cross-shore sediment-partitioning model, Earth Surface Dynamics, 9(2), 183-203, 2021.

705 Clark, J.S.: Dynamism in the Barrier-Beach Vegetation of Great South Beach, New York, Ecological Monographs, 56(2), 97-126, 1986.

Cooper, J.A.G., Green, A.N. and Loureiro, C.: Geological constraints on mesoscale coastal barrier behaviour, Global and Planetary Change, 168, 15-34, 2018.

Cooper, J.A.G., Masselink, G., Coco, G., Short, A.D., Castelle, B., Rogers, K., Anthony, E., Green, A.N., Kelley, J.T.,
710 Pilkey, O.H. and Jackson, D.W.T.: Sandy beaches can survive sea-level rise, Nature Climate Change, 10(11), 993-995, 2020.

Davis, R.A.: Barrier island systems—a geologic overview, in: Geology of Holocene barrier island systems, Springer, Berlin Heidelberg, 1-46, 1994.

Dolan, R.: Barrier dune system along the Outer Banks of North Carolina: a reappraisal, Science, 176(4032), 286-288, 1972.

Elko, N., Briggs, T.R., Benedet, L., Robertson, Q., Thomson, G., Webb, B.M. and Garvey, K.: A century of US beach
715 nourishment, Ocean & Coastal Management, 199, 2021.

FitzGerald, D.M.: Shoreline erosional-depositional processes associated with tidal inlets, in: Hydrodynamics and sediment dynamics of tidal inlets, Springer, New York, 186-225, 1988.

Forde, A.S., Bernier, J.C., and Miselis, J.L.: Archive of ground penetrating radar and differential global positioning system data collected in April 2016 from Fire Island, New York: U.S. Geological Survey data release,
720 https://doi.org/10.5066/F7P84B1P, 2018a.

Forde, A.S., Bernier, J.C., and Miselis, J.L.: Ground penetrating radar and differential global positioning system data collected in April 2016 from Fire Island, New York: U.S. Geological Survey Data Series 1078, https://doi.org/10.3133/ds1078, 2018b.

Forde, A.S., Bernier, J.C., Ciarletta, D.J., and Miselis, J.L.: Ground penetrating radar and global positioning system data
725 collected in 2021 from Fire Island, New York: U.S. Geological Survey data release, https://doi.org/10.5066/P97YW2UL, 2023.

Fuller, M.L.: The geology of Long Island, New York: US Geol. Survey Prof. Paper, 82(231), 1937 p., 1914.

Goldstein, E.B., and Moore, L.J.: Stability and bistability in a one-dimensional model of coastal foredune height, Journal of Geophysical Research: Earth Surface, 121(5), 964-977, 2016.

730   Hapke, C.J., Lentz, E.E., Gayes, P.T., McCoy, C.A., Hehre, R., Schwab, W.C., and Williams, S.J.: A review of sediment budget imbalances along Fire Island, New York: can nearshore geologic framework and patterns of shoreline change explain the deficit? Journal of Coastal Research, 26(3), 510-522, 2010.

Hein, C.J., Fallon, A.R., Rosen, P., Hoagland, P., Georgiou, I.Y., FitzGerald, D.M., Morris, M., Baker, S., Marino, G.B. and Fitzsimons, G.: Shoreline dynamics along a developed river mouth barrier island: Multi-decadal cycles of erosion and event-
735   driven mitigation, Frontiers in Earth Science, 7, 103, 2019.

Hijma, M.P., and Cohen, K.M.: Timing and magnitude of the sea-level jump preluding the 8200 yr event, Geology, 38(3), 275-278, 2010.

Himmelstoss, E.A., Kratzmann, M., Hapke, C., Thieler, E.R., and List, J.: The national assessment of shoreline change: A GIS compilation of vector shorelines and associated shoreline change data for the New England and Mid-Atlantic Coasts:
740   U.S. Geological Survey Open-File Report 2010–1119, https://doi.org/10.3133/ofr20101119, 2010.

Howard, A.D.: Hurricane modification of the offshore bar of Long Island, New York, Geographical Review, 29(3), 400-415, 1939.

Jackson, D.W., Costas, S. and Guisado-Pintado, E.: Large-scale transgressive coastal dune behaviour in Europe during the Little Ice Age, Global and Planetary Change, 175, 82-91, 2019.

745   Kana, T.W.: A mesoscale sediment for Long Island, New York, Marine Geology, 126(1-4), 87-100, 1995.

Kombiadou, K., Costas, S., Carrasco, A.R., Plomaritis, T.A., Ferreira, Ó., and Matias, A.: Bridging the gap between resilience and geomorphology of complex coastal systems, Earth-Science Reviews, 198, 102934 , 2019.

Leatherman, S.P. (Ed.): Barrier islands from the Gulf of St. Lawrence to the Gulf of Mexico, New York: Academic Press, 1979a.

750   Leatherman, S.P.: Migration of Assateague Island, Maryland, by inlet and overwash processes, Geology, 7(2), 104-107, 1979b.

Leatherman, S.P., Rice, T.E., and Goldsmith, V.: Virginia barrier island configuration: a reappraisal, Science, 215(4530), 285-287, 1982.

Leatherman, S.P. and Allen, J.R.: Geomorphic analysis: Fire Island Inlet to Montauk Point, Long Island, New York, Final
755   Report: Reformulation Study for US Army Corps of Engineers, New York District, 1985.

Leatherman, S.P.: Geomorphic and stratigraphic analysis of Fire Island, New York, Marine Geology, 63(1-4), 173-195, 1985.

Leatherman, S.P.: Annotated chronological bibliography of barrier island migration, Journal of Coastal Research, 3(1), 1-14, 1987.

760 Leatherman, S.P.: Role of inlets in geomorphic evolution of the south shore barriers of Long Island, New York, USA, Environmental Management, 13(1), 109-115, 1989.

Lentz, E.E. and Hapke, C.J.: Geologic framework influences on the geomorphology of an anthropogenically modified barrier island: assessment of dune/beach changes at Fire Island, New York, Geomorphology, 126(1-2), 82-96, 2011.

Locker, S.D., Hine, A.C. and Brooks, G.R.: Regional stratigraphic framework linking continental shelf and coastal
765 sedimentary deposits of west-central Florida, Marine Geology, 200(1-4), 351-378, 2003.

Locker, S.D., Miselis, J.L., Buster, N.A., Hapke, C.J., Wadman, H.M., McNinch, J.E., Forde, A.S. and Stalk, C.A.: Nearshore sediment thickness, Fire Island, New York, https://doi.org/10.3133/ofr20171024, 2017.

Lorenzo-Trueba, J. and Ashton, A.D.: Rollover, drowning, and discontinuous retreat: Distinct modes of barrier response to sea-level rise arising from a simple morphodynamic model, Journal of Geophysical Research: Earth Surface, 119(4), pp.779-
770 801, 2014.

Lorenzo-Trueba, J. and Mariotti, G.: Chasing boundaries and cascade effects in a coupled barrier-marsh-lagoon system, Geomorphology, 290, 153-163, 2017.

Ludka, B.C., Guza, R.T., and O'Reilly, W.C.: Nourishment evolution and impacts at four southern California beaches: A sand volume analysis, Coastal Engineering, 136, 96-105, 2018.

775 Magliocca, N.R., McNamara, D.E. and Murray, A.B.: Long-term, large-scale morphodynamic effects of artificial dune construction along a barrier island coastline, Journal of Coastal Research, 27(5), 918-930, 2011.

Malamud-Roam, F. and Ingram, B.L.: Carbon isotopic compositions of plants and sediments of tide marshes in the San Francisco Estuary, Journal of Coastal Research, 17-29, 2001.

Mallinson, D. J., Smith, C. W., Culver, S. J., Riggs, S. R., and Ames, D.: Geological characteristics and spatial distribution
780 of paleo-inlet channels beneath the Outer Banks barrier islands, North Carolina, USA, Estuarine, Coastal and Shelf Science, 88(2), 175-189, 2010.

Mariotti, G. and Hein, C.J.: Lag in response of coastal barrier-island retreat to sea-level rise, Nature Geoscience, 15(8), 633-638, 2022.

Masselink, G., and Lazarus, E.D.: Defining Coastal Resilience, Water, 11(12), 2587, 2019.

785 McBride, R.A., Byrnes, M., and Hiland, M.W.: Geomorphic response-type model for barrier coastlines: a regional perspective, Marine Geology, 126(1-4), 143-159, 1995.

McBride, R.A., Anderson, J.B., Buynevich, I.V., Byrnes, M.R., Cleary, W., Fenster, M.S., FitzGerald, D.M., Hapke, C.J., Harris, M.S., Hein, C.J., Johnson, C.L., Klein, A.H.F., Liu, B., de Menezes, J.T., Mulhern, J.S., Oliver, T.S.N., Pejrup, M., Riggs, S.R., Roberts, H.H., Rodriguez, A.B., Seminack, C.T., Short, A.D., Stone, G.W., Tamura, T., Wallace, D.J., and
790 Wang, P.: Morphodynamics of Modern and Ancient Barrier Systems: An Updated and Expanded Synthesis, in: Treatise on Geomorphology 2nd Edition, edited by: Shroder, J.F., Academic Press, ISBN 978-0-12-818235-2, 2022.

McCormick, L., Neal, W.J. and Pilkey, O.H.: Living with Long Island's south shore, Duke University Press, 1984.

Mendes, V.R. and Giannini, P.C.F.: Coastal dunefields of south Brazil as a record of climatic changes in the South American Monsoon System, Geomorphology, 246, 22-34, 2015.

795 Miselis, J.L., and Lorenzo-Trueba, J.: Natural and human-induced variability in barrier-island response to sea level rise, Geophysical Research Letters, 44(23), 11-922, 2017.

Morang, A.: Shinnecock Inlet, New York, Site Investigation Report 1 Morphology and Historical Behavior, Army Engineer Waterways Experiment Station, Vicksburg, MS, 1999.

Mukhopadhyay, S., Sen, A., Koley, A., and Samanta, P.: Evaluating the formative and shape-controlled dispersive
800 mechanisms of mud balls in a low-energy coastal setting: New insights, Geological Journal, 57(3), 925-949, 2022.

Nienhuis, J.H. and Lorenzo-Trueba, J.: Can barrier islands survive sea-level rise? Quantifying the relative role of tidal inlets and overwash deposition, Geophysical Research Letters, 46(24), 14613-14621. 2019.

Nooren, K., Hoek, W.Z., Winkels, T., Huizinga, A., Van der Plicht, H., Van Dam, R.L., Van Heteren, S., Van Bergen, M.J., Prins, M.A., Reimann, T. and Wallinga, J.: The Usumacinta–Grijalva beach-ridge plain in southern Mexico: a high-
805 resolution archive of river discharge and precipitation, Earth Surface Dynamics, 5(3), 529-556, 2017.

Nordstrom, K.F. and Jackson, N.L.: Bay Shoreline Physical Processes (Fire Island National Seashore Synthesis Paper). Boston: National Park Service Technical Report NPS, NER/NRTR-2005/020, 37p, 2005.

Oliver, T.S., Tamura, T., Short, A.D. and Woodroffe, C.D.: Rapid shoreline progradation followed by vertical foredune building at Pedro Beach, southeastern Australia, Earth Surface Processes and Landforms, 44(2), 655-666, 2019.

810 Passeri, D.L., Dalyander, P.S., Long, J.W., Mickey, R.C., Jenkins III, R.L., Thompson, D.M., Plant, N.G., Godsey, E.S. and Gonzalez, V.M.: The roles of storminess and sea level rise in decadal barrier island evolution, Geophysical Research Letters, 47(18), p.e2020GL089370, 2020.

Price, W.A.: Sedimentology and Quaternary Geomorphology of South Texas Supplementary to Field Trip Manual "Sedimentology of South Texas" Corpus Christi Geological Society Spring Field Trip 1958, Gulf Coast Association of
815 Geological Societies Transactions, 8, 41-75, 1958.

Psuty, N.P.: The coastal foredune: a morphological basis for regional coastal dune development, in: Coastal Dunes, Springer, Berlin, Heidelberg, 11-27, 2008.

Raff, J.L., Shawler, J.L., Ciarletta, D.J., Hein, E.A., Lorenzo-Trueba, J. and Hein, C.J.: Insights into barrier-island stability derived from transgressive/regressive state changes of Parramore Island, Virginia, Marine Geology, 403, 1-19, 2018.

820 Rampino, M.R. and Sanders, J.E.: Holocene transgression in south-central Long Island, New York, Journal of Sedimentary Research, 50(4), 1063-1079, 1980.

Rampino, M.R. and Sanders, J.E.: Evolution of the barrier islands of southern Long Island, New York, Sedimentology, 28(1), 37-47, 1981.

Rampino, M.R. and Sanders, J.E.: Holocene transgression in south-central Long Island, New York: reply, Journal of
825 Sedimentary Research, 52(3), 1982.

Rampino, M.R. and Sanders, J.E.: Barrier island evolution in response to sea-level rise: reply, Journal of Sedimentary Research, 53(3), 1983.

Ramsey, C.B.: Bayesian analysis of radiocarbon dates, Radiocarbon, 51(1), 337-360, 2009.

Reimer, P.J., Austin, W.E., Bard, E., Bayliss, A., Blackwell, P.G., Ramsey, C.B., Butzin, M., Cheng, H., Edwards, R.L.,
830 Friedrich, M. and Grootes, P.M.: The IntCal20 Northern Hemisphere radiocarbon age calibration curve (0–55 cal kBP), Radiocarbon, 62(4), 725-757, 2020.

Rice, T.: Habitat modifications in the US Atlantic coast breeding range of the piping plover (Charadrius melodus) prior to hurricane sandy: A synthesis of tidal inlet and sandy beach habitat inventories, Report submitted to the US Fish and Wildlife Service, 2015.

835 Robbins, M.G., Shawler, J.L. and Hein, C.J.: Contribution of longshore sand exchanges to mesoscale barrier-island behavior: Insights from the Virginia Barrier Islands, US East Coast, Geomorphology, 403 (108163), 2022.

Rogers, L.J., Moore, L.J., Goldstein, E.B., Hein, C.J., Lorenzo-Trueba, J. and Ashton, A.D.: Anthropogenic controls on overwash deposition: Evidence and consequences, Journal of Geophysical Research: Earth Surface, 120(12), 2609-2624, 2015.

840 Ruhfel, A.: Fire Island Inlet, Long Island Forum (May), pp. 89-93, 1971.

Sanders, J.E. and Kumar, N.: Evidence of shoreface retreat and in-place "drowning" during Holocene submergence of barriers, shelf off Fire Island, New York, Geological Society of America Bulletin, 86(1), 65-76, 1975.

Schmelz, W.J. and Psuty, N.P.: Application of geomorphological maps and LiDAR to volumetrically measure coastal geomorphological change from Hurricane Sandy at Fire Island National Seashore. Geomorphology, 408 (108262), 2022.

845 Schubert, C.E.: Analysis of the shallow groundwater flow system at Fire Island National Seashore, Suffolk County, New York: U.S. Geological Survey Scientific Investigations Report 2009–5259, 106 p. https://pubs.usgs.gov/sir/2009/5259/, 2010.

Schupp, C.A., Winn, N.T., Pearl, T.L., Kumer, J.P., Carruthers, T.J., and Zimmerman, C.S.: Restoration of overwash processes creates piping plover (Charadrius melodus) habitat on a barrier island (Assateague Island, Maryland), Estuarine,
850 Coastal and Shelf Science, 116, 11-20, 2013.

Schwab, W.C., Thieler, E.R., Allen, J.R., Foster, D.S., Swift, B.A., and Denny, J.F.: Influence of inner-continental shelf geologic framework on the evolution and behavior of the barrier-island system between Fire Island Inlet and Shinnecock Inlet, Long Island, New York, Journal of Coastal Research, 408-422, 2000.

Schwab, W.C., Baldwin, W.E., Denny, J.F., Hapke, C.J., Gayes, P.T., List, J.H., and Warner, J.C.: Modification of the
855 Quaternary stratigraphic framework of the inner-continental shelf by Holocene marine transgression: An example offshore of Fire Island, New York, Marine Geology, 355, 346-360, 2014.

Schwab, W.C., Baldwin, W.E., Hapke, C.J., Lentz, E.E., Gayes, P.T., Denny, J.F., List, J.H. and Warner, J.C.: Geologic evidence for onshore sediment transport from the inner continental shelf: Fire Island, New York, Journal of Coastal Research, 29(3), 526-544, 2013.

860 Seminack, C.T. and McBride, R.A.: Geomorphic history and diagnostic features of former tidal inlets along Assateague Island, Maryland-Virginia: A life-cycle model for inlets along a wave dominated barrier islands, Shore and Beach, 83(3), 3-24, 2015.

Seneviratne, S.I., Zhang, X., Adnan, M., Badi, W., Dereczynski, C., Di Luca, A., Ghosh, S., Iskandar, I., Kossin, J., Lewis, S., Otto, F., Pinto, I., Satoh, M., Vicente-Serrano, S.M., Wehner, M., and Zhou, B.: Weather and Climate Extreme Events in a Changing Climate, in: Climate Change 2021: The Physical Science Basis. Contribution of Working Group I to the Sixth Assessment Report of the Intergovernmental Panel on Climate Change, Cambridge University Press, doi:10.1017/9781009157896.013, 2021.

Shawler, J.L., Ciarletta, D.J., Connell, J.E., Boggs, B.Q., Lorenzo-Trueba, J. and Hein, C.J.: Relative influence of antecedent topography and sea-level rise on barrier-island migration, Sedimentology, 68(2), 639-669, 2021a.

Shawler, J.L., Ciarletta, D.J., Lorenzo-Trueba, J. and Hein, C.J.: Drowned foredune ridges as evidence of pre-historical barrier-island state changes between migration and progradation, in: Coastal Sediments 2019: Proceedings of the 9th International Conference, 158-171, https://doi.org/10.1142/9789811204487_0015, 2019.

Shawler, J.L., Hein, C.J., Obara, C.A., Robbins, M.G., Huot, S. and Fenster, M.S.: The effect of coastal landform development on decadal-to millennial-scale longshore sediment fluxes: Evidence from the Holocene evolution of the central mid-Atlantic coast, USA. Quaternary Science Reviews, 267, 2021b.

Sherman, D.J.: Problems of scale in the modeling and interpretation of coastal dunes, Marine Geology, 124, 339–349, 1995.

Sirkin, L.A.: Origin and history of maple bog in the Sunken Forest, Fire Island, New York, Bulletin of the Torrey Botanical Club, 131-135, 1972.

Smith, B.N. and Epstein, S.: Two categories of 13C/12C ratios for higher plants, Plant physiology, 47(3), 380-384, 1971.

Strong, J.A.: America's Early Whalemen: Indian Shore Whalers on Long Island 1650–1750, University of Arizona Press, 2018.

Stutz, M.L. and Pilkey, O.H.: A review of global barrier island distribution, Journal of Coastal Research (ICS 2000 Proceedings), 15-22, 2001.

Stutz, M.L. and Pilkey, O.H.: The relative influence of humans on barrier islands: Humans versus geomorphology, Humans as Geologic Agents, 16, 137-147, 2005.

Suydam, C.: Fire Island's Changing Lines, Long Island Forum (April), 73-74, 1942.

Taney, N.E.: Geomorphology of the south shore of Long Island, New York (Technical Memorandum No. 128), US Beach Erosion Board, 1961.

Tanner, B.R., Uhle, M.E., Kelley, J.T. and Mora, C.I.: C3/C4 variations in salt-marsh sediments: An application of
890 compound specific isotopic analysis of lipid biomarkers to late Holocene paleoenvironmental research, Organic
Geochemistry, 38(3), 474-484, 2007.

Tenebruso, C., Lorenzo-Trueba, J., Nichols-O'Neill, S., Ciarletta, D.J., and Miselis, J.L.: The effect of development and
coastal engineering on the evolution of a barrier-marsh-lagoon system: Insights from Long Beach Island, New Jersey,
Frontiers in Earth Science. https://doi.org/10.3389/fmars.2022.958573, 2022.

895 Terrano, J.F., Smith, K.E.L., Bendik, K.J., and Vargas, J.M.: Historical shorelines for Fire Island and Great South Bay, New
York (1834 to 1875): Georeferenced topographic sheets and vector digital data: U.S. Geological Survey data release.
https://doi.org/10.5066/P9LMOCJ0, 2020.

Timmons, E.A., Rodriguez, A.B., Mattheus, C.R. and DeWitt, R.: Transition of a regressive to a transgressive barrier island
due to back-barrier erosion, increased storminess, and low sediment supply: Bogue Banks, North Carolina, USA, Marine
900 Geology, 278(1-4), 100-114, 2010.

U.S. Army Corps.: 2020 USACE NAN Topobathy Lidar DEM: New Jersey and New York.
https://www.fisheries.noaa.gov/inport/item/58880, 2021.

USDA NAIP: Coastal New York NAIP Digital Ortho Photo Imagery,
https://coast.noaa.gov/htdata/raster3/imagery/NY_NAIP_2015_8402/2015_ny_naip.html, 2015.

905 van Ormondt, M., Nelson, T.R., Hapke, C.J. and Roelvink, D.: Morphodynamic modelling of the wilderness breach, Fire
Island, New York. Part I: Model set-up and validation, Coastal Engineering, 157 (103621), 2020.

Vousdoukas, M.I., Ranasinghe, R., Mentaschi, L., Plomaritis, T.A., Athanasiou, P., Luijendijk, A. and Feyen, L.: Sandy
coastlines under threat of erosion, Nature climate change, 10(3), 260-263, 2020.

Williams, J.R., Dellapenna, T.M. and Lee, G.H.: Shifts in depositional environments as a natural response to anthropogenic
910 alterations: Nakdong Estuary, South Korea, Marine Geology, 343, 47-61, 2013.

Williams, J.W. and Jackson, S.T.: Novel climates, no-analog communities, and ecological surprises, Frontiers in Ecology
and the Environment, 5(9), 475-482, 2007.

Zeigler, S.L., Gutierrez, B.T., Lentz, E.E., Plant, N.G., Sturdivant, E.J. and Doran, K.S.: Predicted Sea-Level Rise-Driven
Biogeomorphological Changes on Fire Island, New York: Implications for People and Plovers, Earth's Future, 10(4),
915 p.e2021EF002436, 2022.

Zhang, K. and Leatherman, S.: Barrier island population along the US Atlantic and Gulf Coasts, Journal of Coastal Research, 27(2), 356-363, 2011.

920 **Table 1. Radiocarbon samples obtained from core sites on Fire Island. Sample ID indicates depth with respect to land surface. Inferred environment based on isotope analysis of measured/modeled values from Chmura and Aharon (1995).**

> **Commented [DC1]:** Added conventional dates CE to table

Core ID / Depth	Lab No.	Material	Conventional Age	Con. Date	Calibrated Date / Age		IRMS δ¹³C	Inferred Environment
C1, 121-123 cm	621034	plant material	140 +/- 30 BP	c. 1810 CE	(58.2%) 1797 - 1944 cal CE (37.2%) 1671 - 1779 cal CE	(153 - 6 cal BP) (279 - 171 cal BP)	-28.3 o/oo	Long-lived upland bog / interdune swale or high barrier flat; overlying stratigraphy indicates buried by washover
	638248	**organic sediment**	**330 +/- 30 BP**	**c. 1620 CE**	**(95.4%) 1480 - 1640 cal CE**	**(470 - 310 BP)**	**-28.1 o/oo**	
C3, 99-101 cm	621035	plant material	460 +/- 30 BP	c. 1490 CE	(95.4%) 1412 - 1471 cal CE	(538 - 479 cal BP)	-25.3 o/oo	Long-lived upland bog / interdune swale; overlying stratigraphy indicates buried by washover
	638249	**organic sediment**	**690 +/- 30 BP**	**c. 1260 CE**	**(65.5%) 1272 - 1317 cal CE** **(29.9%) 1360 - 1388 cal CE**	**(678 - 633 cal BP)** **(590 - 562 BP)**	**-26.6 o/oo**	
C7, 51-56 cm	633957	plant material	30 +/- 30 BP	c. 1920 CE	(35.8%) 1867 - 1917 cal CE (31%) 1810 - 1862 cal CE (28.6%) 1694 - 1725 cal CE	(83 - 33 cal BP) (140 - 88 cal BP) (256 - 225 cal BP)	-21.7 o/oo	High marsh; overlying stratigraphy indicates buried by washaround deposition
	638250	**organic sediment**	**140 +/- 30 BP**	**c. 1810 CE**	**(58.2%) 1797 - 1944 cal CE** **(37.2%) 1671 - 1779 cal CE**	**(153 - 6 cal BP)** **(279 - 171 cal BP)**	**-21.7 o/oo**	
C7, 65.5-71 cm	633958	plant material	180 +/- 30 BP	c. 1770 CE	(49.9%) 1722 - 1814 cal CE (19.2%) 1656 - 1698 cal CE (19%) 1910 - Post CE 1950 (7.3%) 1836 - 1880 cal CE	(228 - 136 BP) (294 - 252 BP) (40 - Post BP 0) (114 - 70 BP)	-22.4 o/oo	Brackish fringe; likely undergoing passive drowning based on up-core δ¹³C
	635979	**organic sediment**	**270 +/- 30 BP**	**c. 1680 CE**	**(45.3%) 1618 - 1670 cal CE** **(42.7%) 1508 - 1594 cal CE** **(7%) 1780 - 1798 cal CE** **(0.4%) 1946 - Post CE 1950**	**(332 - 280 BP)** **(442 - 356 BP)** **(170 - 152 cal BP)** **(4 - Post BP 0)**	**-23.4 o/oo**	
C8, 105-111 cm	633959	plant material	130 +/- 30 BP	c. 1820 CE	(64%) 1798 - 1942 cal CE (26.8%) 1674 - 1744 cal CE (4.1%) 1750 - 1765 cal CE (0.5%) 1774 - 1776 cal CE	(152 - 8 cal BP) (276 - 206 cal BP) (200 - 185 cal BP) (176 - 174 cal BP)	-13.2 o/oo	Low marsh; overlying stratigraphy indicates buried by washover
	638251	**organic sediment**	**280 +/- 30 BP**	**c. 1670 CE**	**(54.7%) 1504 - 1596 cal CE** **(37.7%) 1616 - 1666 cal CE** **(3%) 1783 - 1795 cal CE**	**(446 - 354 cal BP)** **(334 - 284 cal BP)** **(167 - 155 cal BP)**	**-16.6 o/oo**	
C8, 111-118 cm	633960	plant material	180 +/- 30 BP	c. 1770 CE	(49.9%) 1722 - 1814 cal CE (19.2%) 1656 - 1698 cal CE (19%) 1910 - Post CE 1950 (7.3%) 1836 - 1880 cal CE	(228 - 136 BP) (294 - 252 BP) (40 - Post BP 0) (114 - 70 BP)	-11.5 o/oo	High marsh; likley undergoing passive drowning based on up-core δ¹³C; plant material may include roots from overlying low marsh or record high to low marsh transition in-situ
	638252	**organic sediment**	**260 +/- 30 BP**	**c. 1690 CE**	**(51.5%) 1620 - 1674 cal CE** **(28.7%) 1516 - 1590 cal CE** **(13.6%) 1766 - 1800 cal CE** **(1.6%) 1942 - Post CE 1950**	**(330 - 276 BP)** **(434 - 360 BP)** **(184 - 150 BP)** **(8 - Post BP 0)**	**-21.1 o/oo**	
C9, 57-62 cm	633961	plant material	120 +/- 30 BP	c. 1830 CE	(67.2%) 1799 - 1940 cal CE (25.8%) 1680 - 1740 cal CE (2.4%) 1752 - 1764 cal CE	(151 - 10 cal BP) (270 - 210 cal BP) (198 - 186 cal BP)	-16.1 o/oo	High marsh; possibly burying former low marsh, or including plant debris from adjacent low marsh
	638253	**organic sediment**	**90 +/- 30 BP**	**c. 1860 CE**	**(69.4%) 1806 - 1926 cal CE** **(26%) 1687 - 1730 cal CE**	**(144 - 24 cal BP)** **(263 - 220 cal BP)**	**-21.9 o/oo**	
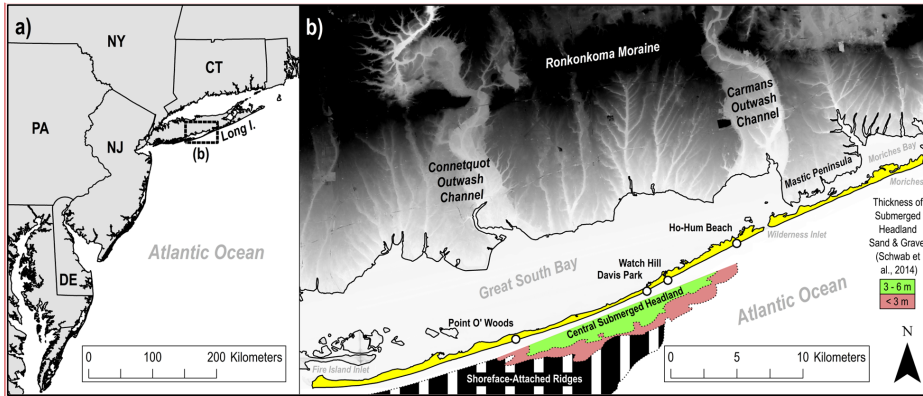
Figure 1: (a) U.S. Mid-Atlantic region—Fire Island is positioned centrally along the southern coast of Long Island, New York (black box; panel b). (b) Detail of Fire Island, highlighted in yellow, and Long Island, depicted in grayscale lidar-derived topography (white = 0 m, black = 35+ m NAVD88). The two most prominent features of the mainland behind Fire Island are the former Connetquot and Carmaens glacial outwash channels, which extend seaward from the Ronkonkoma Moraine. Also shown is an area of shoreface-attached ridges (black and white stripes) and the location and approximate thickness of the Central Submerged Headland (red and green fill)—a shallow Pleistocene sediment lobe that underlies the barrier shoreface between Watch Hill and Point O' Woods. Boundaries and thickness of submerged headland and area of shoreface-attached ridges modified after Schwab et al. (2014). Lidar digital elevation model from FEMA (2006).

925
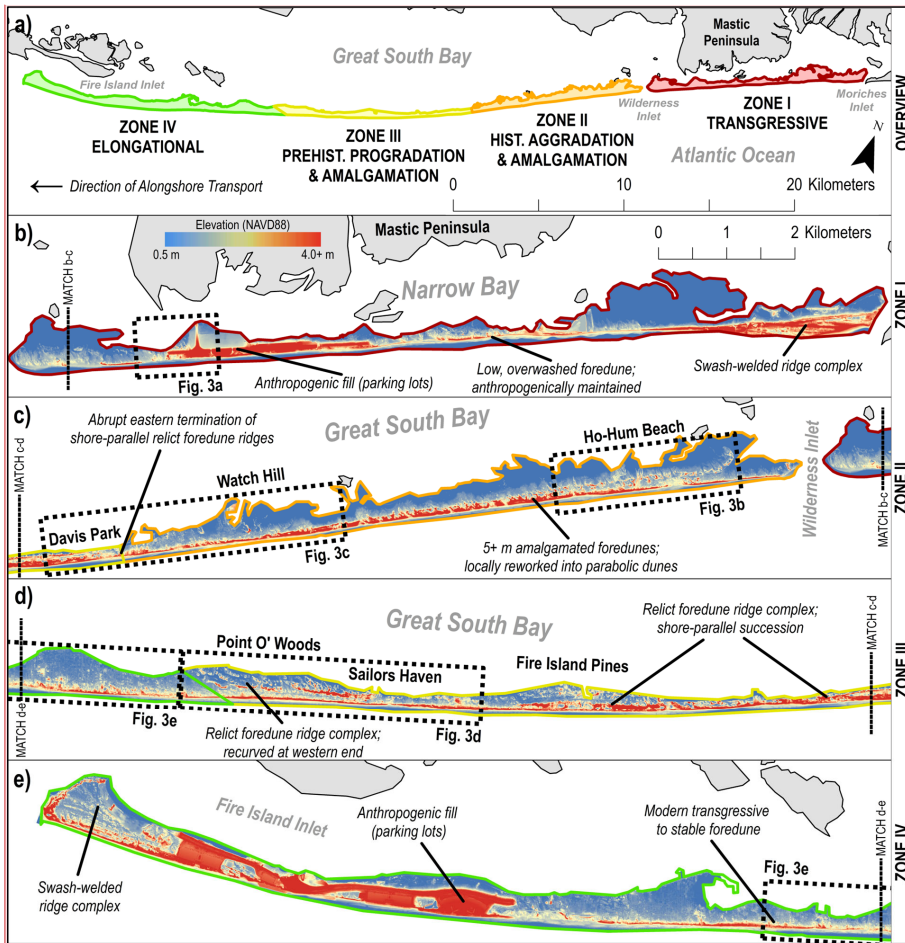
930

Figure 2: (a) Geomorphic zones of Fire Island (modified from Ciarletta et al., 2021), which mirror the east-to-west alongshore transport gradient. **(b)** Transgressive zone (red), which fronts the Mastic Peninsula and has undergone recent and historical erosion and retrogradation. **(c)** Zone of historical (hist.) aggradation and amalgamation (orange), which features 8 m elevation dunes and has undergone recent erosion since the (re)opening of Wilderness Inlet in 2012. **(d)** Zone of prehistoric (preshist.) progradation and 935 amalgamation (yellow), with multiple moderate-relief and shore-parallel dune ridges and relatively stable shoreline positions since the mid-19th century. **(e)** Zone of elongation (green), which has historically elongated westward since at least 1825 and likely earlier. Lidar digital elevation model from Brenner et al. (2016).
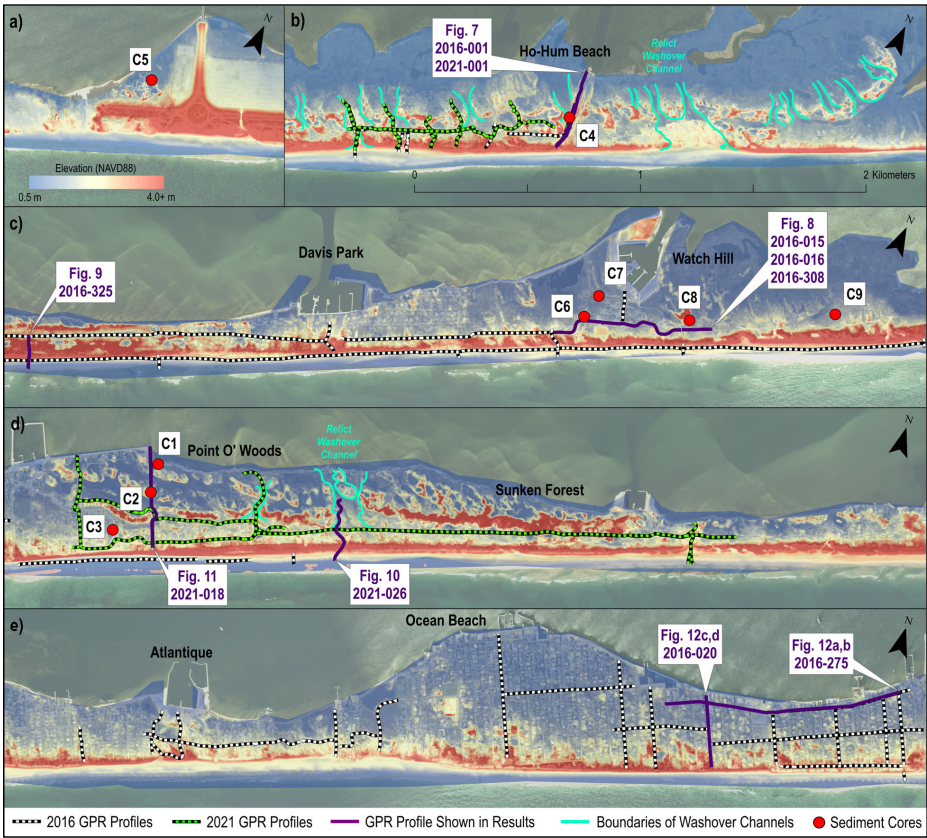
Figure 3: Study sites on/adjacent to central Fire Island, from east to west. Annotated purple lines are ground-penetrating radar transects with profiles shown in Results and Interpretation. Panel (a) depicts the easternmost limit of the Otis Pike Fire Island High Dune Wilderness, just east of Wilderness Inlet, where the barrier transitions to a historically transgressive single-foredune system heavily modified by human intervention. Panel (b) depicts Ho-Hum Beach, which is in the updrift portion of the central region just west of Wilderness Inlet and features a 5-8 m elevation double dune-ridge system. Panel (c) shows the area around Watch Hill and Davis Park, which is at the interface of Zones II and III, and features an anomalous low spot near cores C6 and C7. Finally, panels (d) and (e) depict a 7-km stretch of barrier centered on Point O' Woods. The eastern 4 km of this section is marked by a succession of relict dune ridges that gently recurve and splay to the northwest at Point O' Woods proper. Lidar digital elevation model from Brenner et al. (2016); base imagery USDA NAIP (2015).
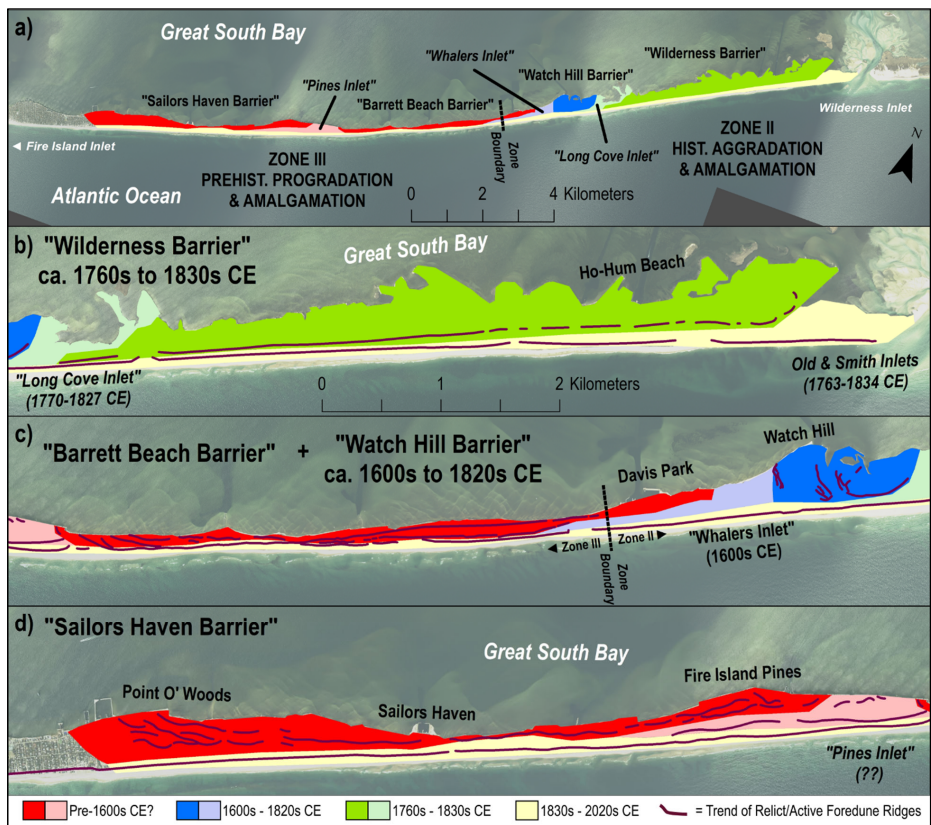
Figure 4: Morphochronological map of central Fire Island, depicting relationships among the relict and modern landforms of the barrier system, with dates from historical observations (McCormick et al., 1984; Strong, 2018); b, c, d at same map scale. Red-hued areas are interpreted as the oldest portions of the barrier platform and comprise two former rotational barrier remnants and an intervening inlet fill—as evidenced by the geometry of relict dune ridges—that predate the historical record. Blue-hued areas are the second-oldest component of the system and correspond with a recurved spit complex and adjacent downdrift inlet at Watch Hill that was historically active at least until 1670 CE. Green-hued areas represent portions of the system that were documented to be historically active from at least the mid-18th century through the early 19th century, while the pale-yellow region corresponds to the extent of the modern foredune, which likely postdates the mid-18th century across most of its length. Base imagery is USDA NAIP (2015).
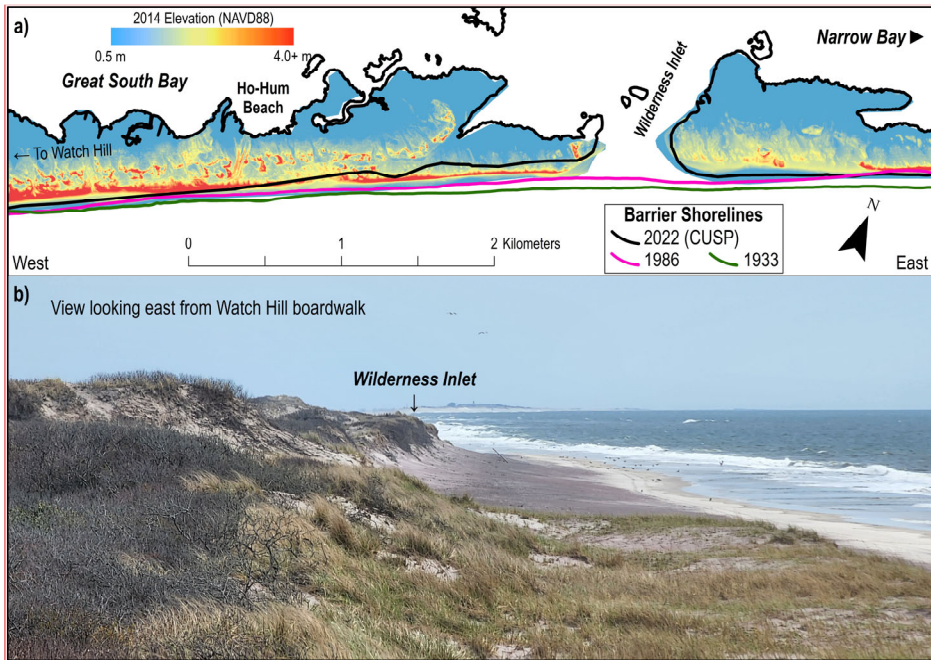
Figure 5: (a) Changes in shoreline geometry at the eastern end of the Wilderness Barrier, overlain on a lidar DEM from 2014 (see Brenner et al., 2016); 1933 and 1986 shorelines from Himmelstoss et al. (2010). The black line outlines the shoreline of Fire Island in 2022, as represented by NOAA's Continually Updated Shoreline Product (CUSP), which is defined as the MHW shoreline as derived from a variety of sources (see https://shoreline.noaa.gov/data/datasheets/cusp.html). Much of the foredune along the 2.5 kilometers of coast downdrift of the Wilderness Inlet has been eroded. (b) View looking east from Watch Hill towards the Wilderness Inlet in April 2022. A prominent offset has developed between the updrift and downdrift coasts bracketing the inlet. Photo credit: D. Ciarletta, USGS.
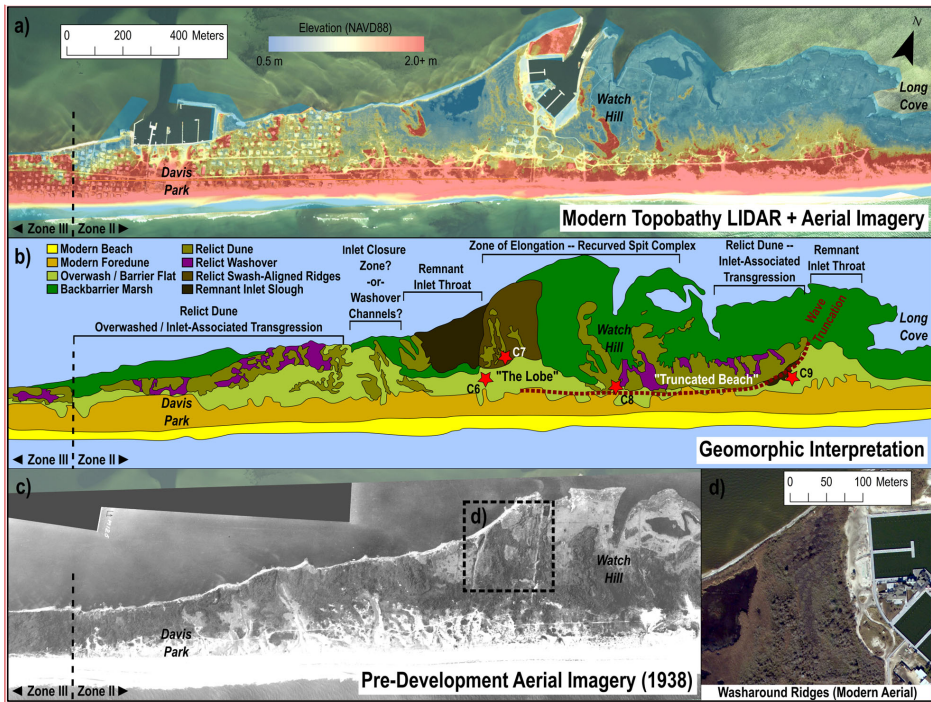
Figure 6: (a) 2014 Lidar ~~digital elevation model~~DEM of the Watch Hill-Davis Park area shaded between 0.5 and 2.0 m elevation to bring out low-relief features (see Brenner et al., 2014) overlain on 2015 NAIP imagery. (b) Detailed morphologic map of the same, showing structure of relict barrier topography and locations of remnant inlet throats. Dashed red line between cores C6 and C9 (red stars) depicts an inferred shoreline probably dating to the early 19th century based on comparison with U.S. Coast and Geodetic Survey Chart H-46, 1835. "Truncated Beach" and "The Lobe" refer to updrift and downdrift complexes of recurved and washaround ridges inferred to exist on distinct depositional platforms within the zone of spit elongation. Their alongshore subsurface structure is shown in Figure 8. (c) Pre-development Beach Erosion Board (U.S. Army Corps) aerial imagery of Davis Park-Watch Hill area, with inset (d) showing presence of washaround ridges ringing a central high point on an abandoned spit deposit—"The Lobe"—updrift of Whalers Inlet (Modern aerial: USDA NAIP, 2015).

970

975
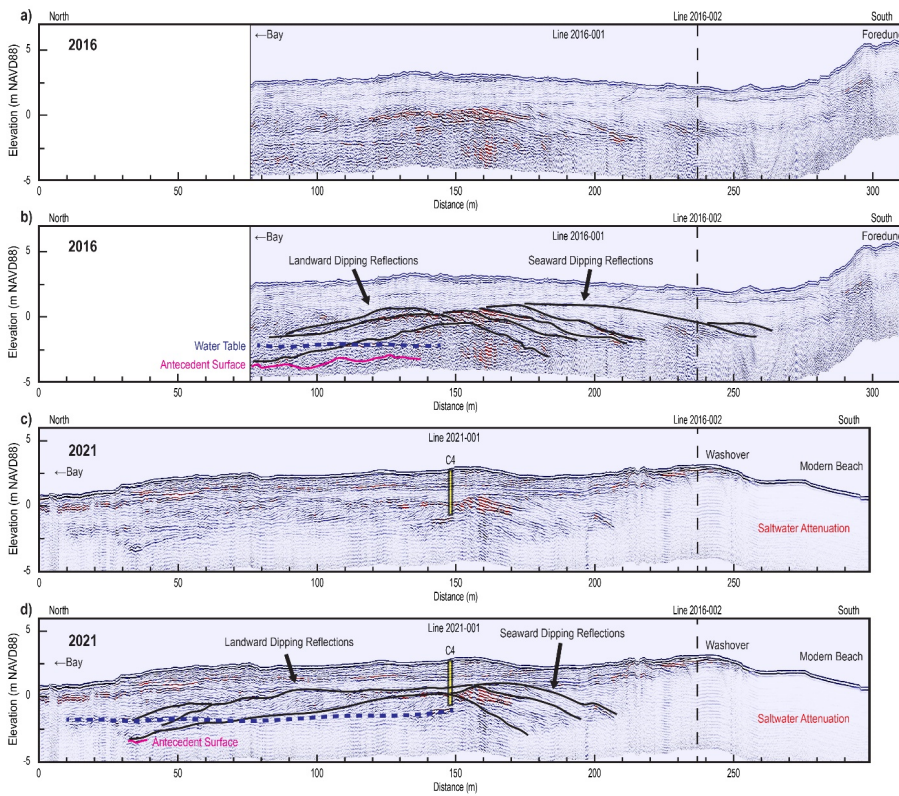
Figure 7: Cross-shore uninterpreted (a, c) and interpreted (b, d) GPR profiles of the same line at Ho-Hum ~~Bb~~each in 2016 (a, b) and 2021 (c, d), showing the structure and lithology of the Wilderness Barrier near the eastern end of Zone II. Black lines highlight prominent reflections within and between presumed washover and beach facies. Seaward-dipping reflections south of Core C4 (panels c, d; yellow) are consistent with past progradation, while landward-dipping reflections to the north highlight relict washover. A gently undulating reflector (magenta) under the landward-dipping units at approximately -3 m elevation may correspond with the antecedent Pleistocene surface. Modern foredune visible at the seaward end of 2016 profile has been destroyed by erosion in 2021, leaving behind only a low, transgressive remnant about 60 m landward of the original dune position.

980
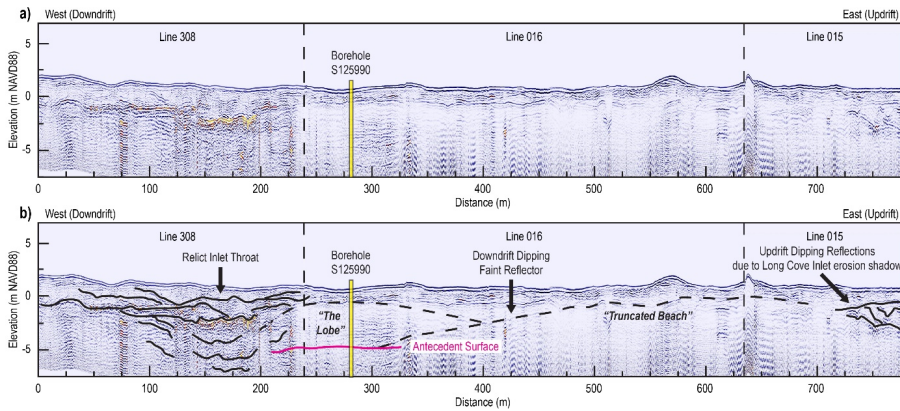
985 **Figure 8: Alongshore uninterpreted (a) and interpreted (b) GPR transect behind the modern foredune at Watch Hill (east/updrift) and the former Whalers Inlet (west/downdrift). Black lines highlight prominent reflections within and between presumed washover, beach, and inlet facies. Scans reveal the structure of the updrift platform of the spit complex, "The Lobe"," upon which cores C6 and C7 are sited, and a relict inlet throat that probably represents the final position of Whalers Inlet. The inlet cuts to an elevation of at least -6 m NAVD88, which is below the depth of the observed transgressive surface underlying the barrier at this location.**

990
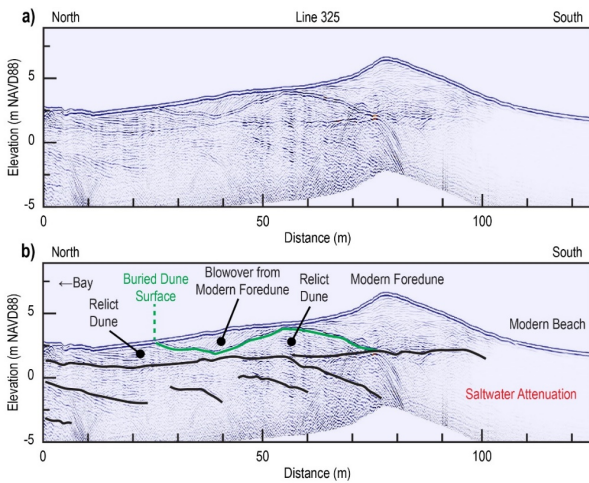
Figure 9: Shore-perpendicular uninterpreted (a) and interpreted (b) GPR transect west of Davis Park, slightly more than 2 km downdrift of the former Whalers Inlet. Black lines highlight prominent reflections within and between presumed washover and beach facies. The profile reveals seaward-dipping reflectors consistent with past progradation of the Barrett Beach Barrier. Above
995 **these reflections, the active foredune has amalgamated against a relict dune line and infilled a relict swale with blowover.**
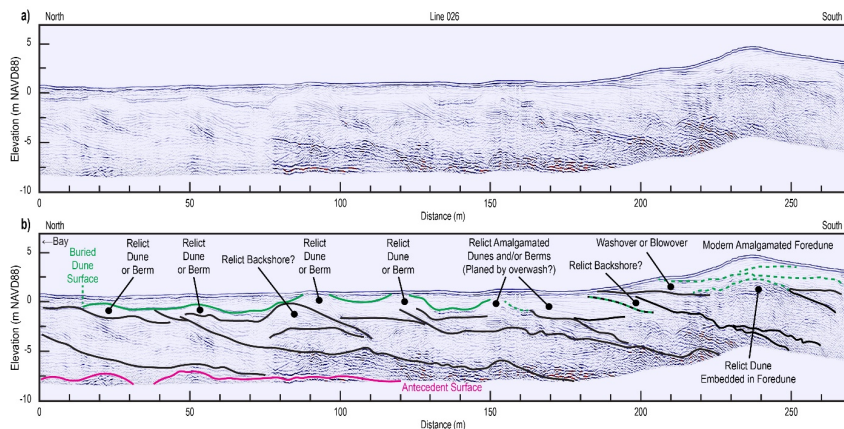
Figure 10: Shore-perpendicular uninterpreted (a) and interpreted (b) GPR transect just east of Point O' Woods, near the Sunken Forest. The profile depicts a 250+ m-wide succession of progradational clinoforms overlying a possible antecedent surface (magenta) at a depth of -7.5 m NAVD88. Low-relief relict dune ridges and possible relict berms are also present in the subsurface behind the landward limit of the modern foredune. Black lines highlight prominent reflections within and between presumed washover and beach facies. Buried dune surfaces are indicated in green, with dashed green lines indicating dune surfaces buried by aeolian amalgamation. The black-and-green dashed line indicates a dune surface buried by possible beach facies.

1000
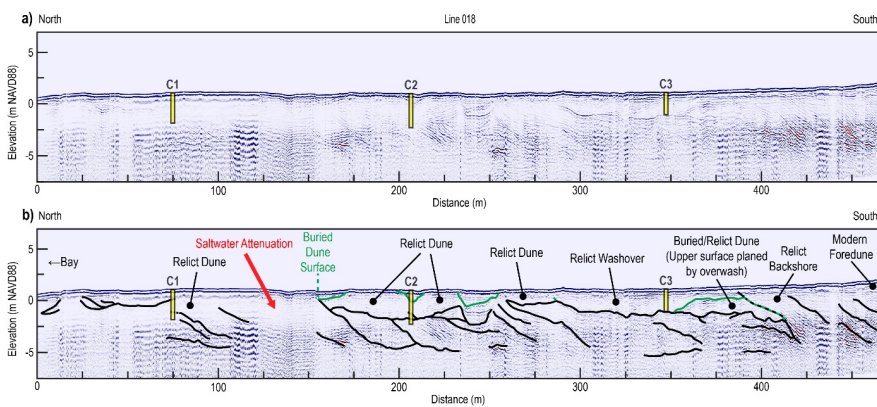
1005 **Figure 11: Cross-shore uninterpreted (a) and interpreted (b) GPR profile at Point O' Woods showing location of sediment vibracores and interpreted stratigraphy based on correlation with cores. The stratigraphic structure of the transect is primarily progradational and features a succession of partly buried relict foredunes. Additionally, there is a possible transgressional dune preserved in the subsurface at ~380 m seaward of the lagoon shoreline. A Wwashover unit overlies the dune and onlaps an interpreted relict swale surface in the landward direction. In the seaward direction, progradational beach clinoforms offlap from the relict dune surface and**

1010 **underlie the heel of the modern foredune. Black lines highlight prominent reflections within and between presumed washover and**

beach facies, while ~~Bb~~uried dune surfaces are indicated in green~~. , and T~~the black-and-green dashed line indicates the dune surface buried by possible beach facies.
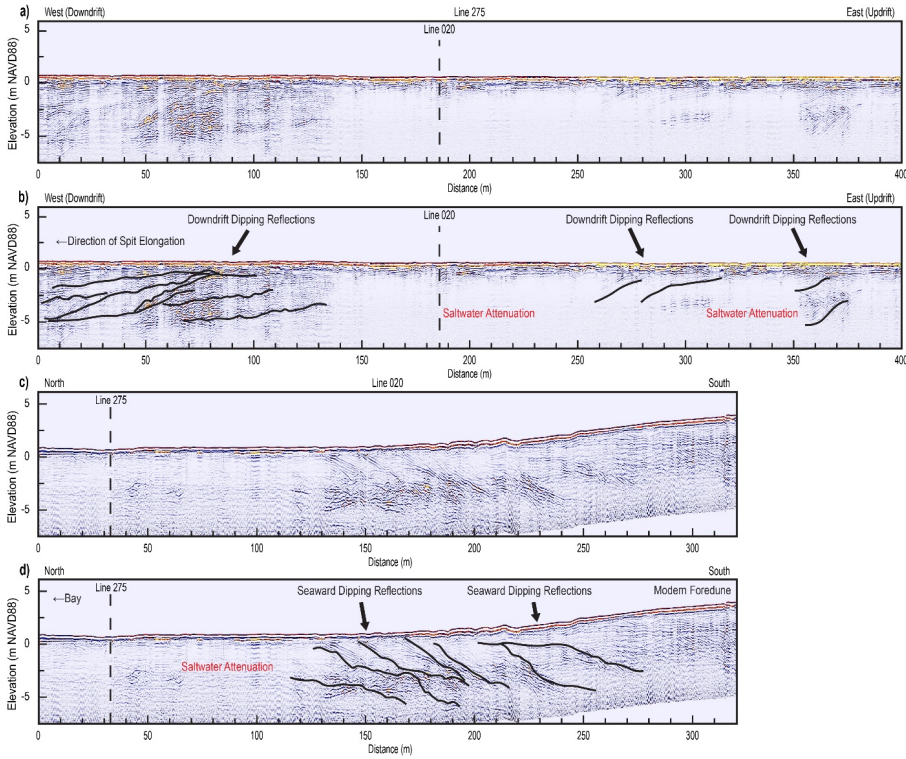
1015   **Figure 12: Uninterpreted (a, c) and interpreted (b, d) GPR transects of intersecting north-south line 20 and east-west line 275, located 2 km downdrift of Point O' Woods (see Figure 3e for location). Black lines highlight prominent reflections within and between presumed washover and beach deposits. ~~SProfiles depict s~~teeply dipping reflections in both the seaward (c/d) and downdrift directions (a/b)~~,~~ are consistent with spit development.**
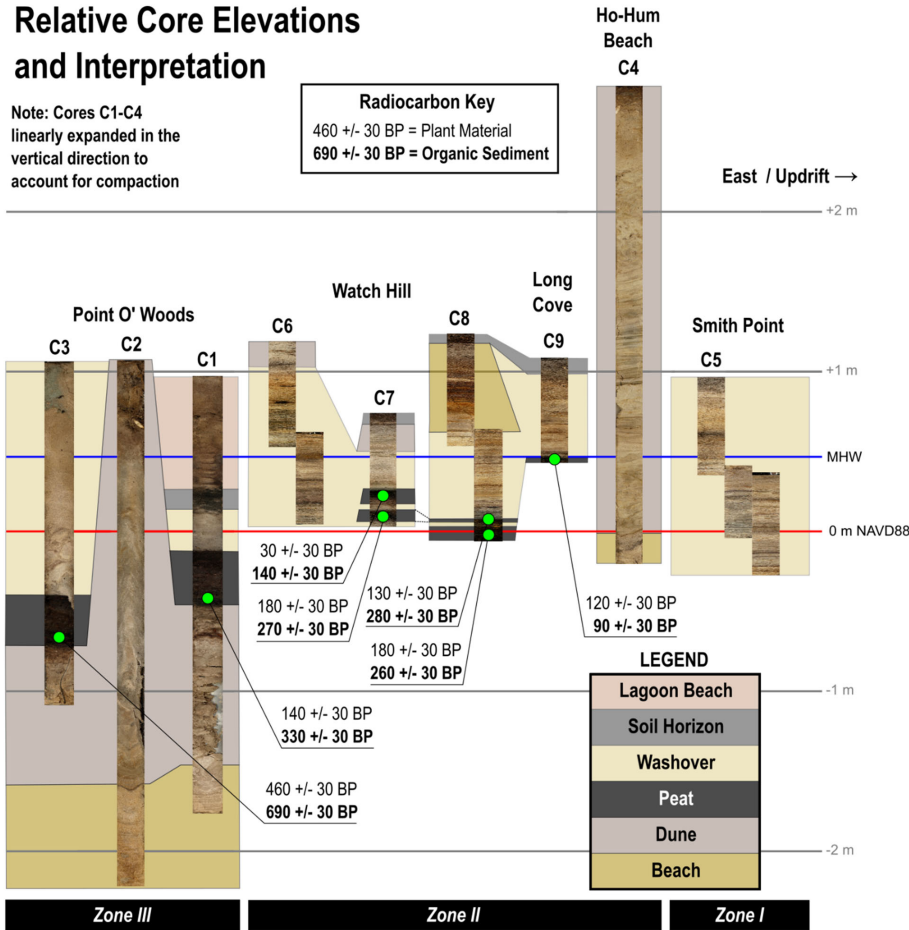
Figure 13: Relative elevations of sediment cores (NAVD88) and interpretation of lithologies. Green dots mark locations of radiocarbon samples, with ages reported for both plant material and organic sediment (see Table 1). Modern mean high water (MHW) is indicated at +0.46 m.

1020
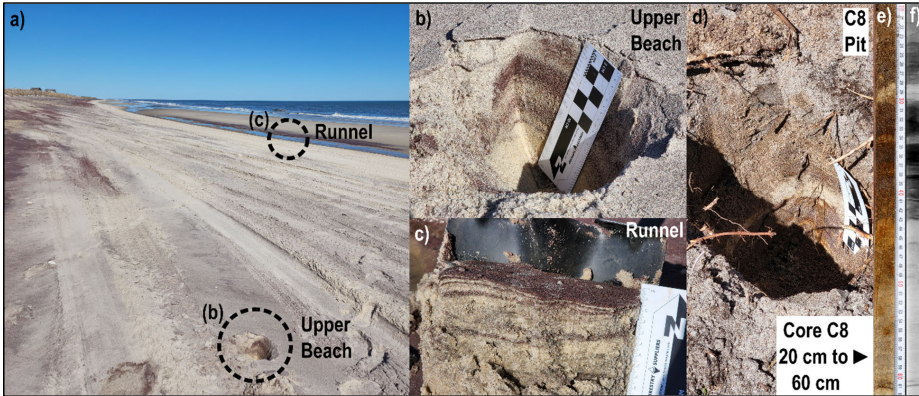
Figure 14: Visual comparison of Ceore C8 with post-storm beach lithology. (a) Overview of beach at Davis Park two days after the April 2022 nor'easter. (b) Small pit dug into modern upper beach, revealing alternating layers of heavy minerals and clean sand. (c) Dug-out section of runnel floor revealing thin, deformed heavy mineral and clean sand bands. (d) Pit at site C8, revealing in-situ lithology comparable to modern beach. (e) Core C8 core section between 20 and 60 cm, showing detailed lithology. Some orange staining is apparent from groundwater. (f) X-ray image of section shown in (e). Darker units contain heavy minerals. Photo credit (a-d): D. Ciarletta, USGS.

Figure 15: Timeline of central Fire Island's evolution from the 16th century to the present, based on a synthesis of geomorphic interpretation and age control from this study, as well as historical accounts and analyses described in previous studies and reports (Clark, 1986; Leatherman and Allen, 1985; McCormick, 1984; Ruhfel, 1971; Suydam, 1942). Compare with Figure 4 for detailed morphochronology, including traces of relict ridges.

1035